NONLINEAR MODEL PREDICTIVE CONTROL BASED FUEL-EFFICIENT ADAPTIVE VEHICLE SPACING STRATEGY FOR HEAVY-DUTY VEHICLE PLATOONING

by

Mert Aygün

B.S., Control and Automation Engineering, Yıldız Technical University, 2019

Submitted to the Institute for Graduate Studies in
Science and Engineering in partial fulfillment of
the requirements for the degree of
Master of Science

Graduate Program in Systems and Control Engineering
Boğaziçi University

2023

ACKNOWLEDGEMENTS

I would like to express my sincere gratitude and appreciation to all those who have supported and contributed to the completion of this master's thesis.

First and foremost, I am deeply grateful to my thesis advisor, Sinan Öncü, for his invaluable guidance, mentorship, and unwavering support throughout the entire research process. His expertise, constructive feedback, and dedication have been instrumental in shaping the direction and quality of this work.

I am grateful to AVL Türkiye for their support in providing me the flexibility to carry out this research. I would like to acknowledge the assistance and cooperation of my colleagues at AVL Türkiye, particularly Ahmet Sakallı and Ferit Hacıoğlu. Their knowledge-sharing, valuable discussions and collaborative spirit have greatly contributed to the success of this thesis.

My heartfelt thanks go to my family and friends for their unconditional love, encouragement, and unwavering support during this challenging period. Their belief in my abilities and constant encouragement have been a tremendous source of motivation throughout the research process.

While it is not possible to mention everyone individually, please know that your contributions, whether big or small, have played a significant role in the successful completion of this thesis.

Thank you all for being a part of this incredible journey.

ABSTRACT

NONLINEAR MODEL PREDICTIVE CONTROL BASED FUEL-EFFICIENT ADAPTIVE VEHICLE SPACING STRATEGY FOR HEAVY-DUTY VEHICLE PLATOONING

This thesis presents an approach for enhancing fuel efficiency in heavy-duty vehicle platooning through the implementation of an adaptive spacing strategy. The optimization design incorporates two crucial components, namely the nonlinear fuel consumption model of a diesel engine and the nonlinear air drag model. By integrating these elements into the overall cost function, a nonlinear model predictive controller is devised to calculate an adaptive time headway strategy. The primary focus is minimizing fuel consumption by adjusting the time headway which also affects the air drag coefficient. However, simply reducing the time headway and the air drag coefficient may not always be the most fuel-efficient strategy. In some scenarios, keeping up to the minimum set time headway can lead to excessive control effort, resulting in higher fuel consumption because the vehicle has to operate its engine within the inefficient fuel map region. The proposed dynamic strategy allows modifying the intervehicular distance within certain boundaries in order to optimize the potential benefits of aerodynamic drag reduction while respecting the engine's fuel map. To assess the effectiveness of the control design and validate the expected outcomes, extensive closed-loop simulations are conducted. A benchmark truck model is utilized, and various road topography conditions involving uphill and downhill slopes are considered. The simulation results underscore the efficacy of the adaptive time headway strategy in reducing fuel consumption for heavy-duty trucks across different scenarios. When compared to the lead vehicle, fuel consumption is reduced by up to 8%, and compared to a constant time headway approach, reductions of up to 3% are observed.

ÖZET

AĞIR YÜK TAŞIYAN ARAÇ KONVOY SİSTEMLERİ İÇİN YAKIT VERİMLİLİĞİ ODAKLI DOĞRUSAL OLMAYAN MODEL ÖNGÖRÜLÜ KONTROLE DAYALI ADAPTİF ARAÇ ARALIĞI STRATEJİSİ

Bu tezin amacı, adaptif bir zaman aralığı stratejisi uygulayarak ağır yük taşıyan araç konvoylarında yakıt verimliliğini artırmayı amaçlayan bir yaklaşım sunmaktır. Optimizasyon tasarımı, temel terimler olarak dizel motorun yakıt tüketiminin ve hava direncinin doğrusal olmayan modellerini içermektedir. Bu unsurlar genel maliyet fonksiyonuna, adaptif bir zaman aralığı stratejisi hesaplamak için entegre edilip doğrusal olmayan bir model öngörülü kontrolör tasarımında kullanılır. Temel odak noktası, zaman aralığını ayarlayarak yakıt tüketimini en aza indirmektir ve bu durum hava direnci katsayısını da etkilemektedir. Ancak, zaman aralığını ve hava direnci katsayısını azaltmak her zaman en verimli yakıt strateji olmayabilir. Bazı senaryolarda, minimum zaman aralığına uymak aşırı kontrol çabasına neden olabilir, bu da aracın motorunu verimsiz yakıt haritası bölgesinde çalıştırmasıyla daha yüksek yakıt tüketimine yol açar. Önerilen dinamik strateji, potansiyel have direnci azaltma avantajlarını optimize etmek için belirli sınırlar içinde araçlar arası mesafeyi değiştirmeye olanak tanırken, motorun yakıt haritasını da dikkate alır. Kontrol tasarımının etkinliğini değerlendirmek ve beklenen sonuçları doğrulamak için kapsamlı kapalı çevrim simülasyonlar yapılmıştır. Bir referans kamyon modeli kullanılmış olup yukarı ve aşağı eğimli çeşitli yol topografyası koşulları dikkate alınmıştır. Simülasyon sonuçları, adaptif zaman aralığı stratejisinin farklı senaryolarda ağır yük taşıyan kamyonların yakıt tüketimini azaltmada etkinliğini vurgulamaktadır. Öncü araçla karşılaştırıldığında, yakıt tüketimi %8'e kadar azaltılmış ve sabit zaman aralığı yaklaşımına kıyasla %3'e varan azalmalar gözlemlenmiştir.

TABLE OF CONTENTS

LIST OF FIGURES

LIST OF TABLES

LIST OF SYMBOLS

a_h	Acceleration of the host vehicle
a_{min}	Minimum achievable acceleration
a_{max}	Maximum achievable acceleration
A_f	Cross-sectional area of the vehicle
C_D	Air drag coefficient
C_D^0	Nominal air drag coefficient
d	Actual distance
d_i	Actual inter-vehicle spacing between (i−1)-th and i-th vehicles
d_{des}	Desired inter-vehicle spacing
d_{min}	Minimum allowed inter-vehicle spacing
d_{max}	Maximum allowed inter-vehicle spacing
e	Distance error
f_0	First rolling resistance coefficient
f_s	Second rolling resistance coefficient
F_b	Brake force
F_a	Aerodynamic drag force
F_r	Rolling resistance force
F_g	Gravitational resistance force
g	Gravitational constant
i	Vehicle index
i_g	Gear ratio
u_b	Brake control input of the benchmark truck model
u_δ	Fuel injection input of the benchmark truck model
u_{egr}	EGR valve input of the benchmark truck model
$u_{g,r}$	Gear request input of the benchmark truck model
u_{vgt}	VGT opening input of the benchmark truck model
m	Vehicle mass
r_w	Wheel radius

M_e	Engine torque
M_w	Wheel torque
x	Vehicle position
$\dot{x}$	Vehicle speed
Q	Traffic flow rate
α_1	First characteristic parameter of air drag function
α_2	Second characteristic parameter of air drag function
$\beta_t(i)$	Backward variable
δ_i	Spacing error of the host vehicle
Δx	Intervehicular distance
ρ	Traffic density
Θ	Parameter set
τ	Time-headway constant
τ_{min}	Minimum time-headway limit
τ_{max}	Maximum time-headway limit
v	Vehicle speed
v_h	Speed of the host vehicle
v_p	Speed of the preceding vehicle
v_{i-1}	Speed of i-th vehicle's predecessor
ω_e	Rotational speed of the engine
ω_w	Rotational speed of the wheel

LIST OF ACRONYMS/ABBREVIATIONS

ACC	Adaptive Cruise Control
ADAS	Advanced Driver Assistance Systems
AHS	Automated Highway Systems
ATH	Adaptive Time Headway
BTM	Benchmark Truck Model
CACC	Cooperative Adaptive Cruise Control
CSP	Constant Spacing Policy
CTH	Constant Time Headway
DP	Dynamic Programming
EGR	Exhaust Gas Recirculation
GCDC	Grand Cooperative Driving Challenge
GPS	Global Positioning System
HDV	Heavy Duty Vehicle
ICE	Internal Combustion Engine
IEEE	Institute of Electrical and Electronics Engineers
LAC	Lookahead Cruise Control
MPC	Model Predictive Control
NMPC	Nonlinear Model Predictive Control
PATH	Partners for Advanced Transit and Highways
PLF	Predecessor Leader Following
PRT	Personal Rapid Transit
SARTRE	Safe Road Trains for the Environment
TCU	Transmission Control Unit
VGT	Variable Geometry Turbocharger
V2V	Vehicle-to-Vehicle
V2I	Vehicle-to-Infrastructure

1. INTRODUCTION

The transportation sector is a major contributor to global greenhouse gas emissions, with heavy-duty vehicles (HDVs) being one of the largest sources of emissions. Road freight transportation is responsible for 15% of all freight activity and accounts for 65% of all total freight CO_2 emissions, as stated in ITF Transport Outlook 2021 [1]. Currently, carbon-neutral solutions for heavy-duty trucks are not widely available and require further technological advancements, supply, and infrastructure [2]. In recent years, researchers and industry professionals have been exploring various approaches to reduce the environmental impact of HDVs, such as improving engine efficiency, using alternative fuels, and optimizing driving behavior [3]. One promising approach is HDV platooning, which has the potential to improve fuel efficiency, reduce emissions, and increase road safety. By allowing HDVs to travel in close proximity to each other, platooning reduces aerodynamic drag, which accounts for about 25% of a truck's fuel consumption [4], and allows for more efficient use of road space. In literature, the experimental studies reported a 10% reduction in fuel consumption [5–7]. Moreover, platooning can enhance the safety of HDV operations by minimizing human error and improving the stability of the vehicles.

1.1. Vehicular Platooning

The concept of vehicle platooning dates back to the early 20th century when the first convoys of military vehicles were formed to transport troops and supplies during wartime. However, it was not until the 1990s that platooning began to be explored as a means of improving fuel efficiency and reducing emissions in commercial transportation. The PATH program (Partners for Advanced Transit and Highways), launched in 1986 by the University of California, Berkeley [8], played a key role in advancing platooning technology through research and development projects in collaboration with industry partners. The earliest experiments involved using advanced sensors and communication systems to allow trucks to follow each other at a short distance while maintaining

a safe speed and trajectory [9] on highways. In the following decades, platooning technologies continued to evolve, with the introduction of automated steering, braking, and acceleration systems.

According to the National Highway Traffic Safety Administration (NHTSA), about 94% of traffic crashes are caused by human error [10]. This includes errors such as distracted driving, speeding, impaired driving, and failure to yield or obey traffic signals. NHTSA believes that advanced driver assistance systems (ADAS) have the potential to reduce the number of crashes caused by human error, but it is important to note that ADAS systems are not perfect and can also have limitations and failures. Ultimately, human drivers are still responsible for safe driving and should not rely solely on ADAS technology to prevent crashes. The SARTRE (Safe Road Trains for the Environment) project [11] was a European Commission-funded research project that aimed to develop and test a road train concept for heavy-duty vehicles, which involves a lead vehicle driven by a professional driver and a platoon of following vehicles driven autonomously by a combination of on-board sensors and vehicle-to-vehicle communication. One of the key safety benefits of the SARTRE road train concept was that it could potentially reduce driver fatigue and distractions, as drivers in the following vehicles could relax and perform other tasks while the vehicle drove autonomously. This could result in a lower risk of accidents caused by human error, such as speeding, distraction, or drowsiness.

Another technology that has been developed to improve the safety and efficiency of heavy-duty vehicle platooning is Cooperative Adaptive Cruise Control (CACC) [12]. CACC builds upon the existing technology of Adaptive Cruise Control (ACC), which uses radar and other sensors to automatically maintain a set distance between vehicles. However, CACC goes beyond ACC by allowing vehicles in a platoon to communicate with each other through vehicle-to-vehicle (V2V) communication. This allows the vehicles to coordinate their movements and speed, which can result in smoother and safer driving. CACC also has the potential to reduce the risk of accidents caused by sudden braking or changes in speed. In a platoon of CACC-equipped vehicles, the lead vehi-

cle would set the speed, and the following vehicles would automatically adjust their speed to maintain a safe distance from the vehicle in front. This would minimize the need for sudden braking and reduce the risk of collisions. While CACC technology has shown promise in improving the safety and efficiency of both homogeneous and heterogeneous [13] vehicle platooning, Grand Cooperative Driving Challenge (GCDC) being one of the endeavors [6, 14], it is important to note that it is still in the development phase and has not yet been widely adopted. Further research and testing are needed to fully understand the technology's potential benefits and limitations to ensure its safe integration into our transportation system.

One important concept in platooning is string stability, which refers to the ability of a platoon to maintain a constant spacing between vehicles without amplifying or dampening any disturbances that may arise in the system. String stability is crucial for ensuring that the platoon remains safe and stable over time [15], even in the presence of external disturbances such as gusts of wind or changes in traffic flow. However, it is not considered in this work since the focused problem consists of a two-vehicle platoon which does not show the propagation of the spacing error leading to an unstable vehicle string.

1.1.1. Necessity for Fuel-Efficient Platooning

Vehicle platooning has demonstrated its effectiveness in minimizing fuel consumption and greenhouse gas emissions. This approach involves operating a cluster of vehicles in close proximity, resulting in reduced aerodynamic drag for the following vehicles. This reduction is attributed to the slipstream effect occurring behind a moving vehicle. As the distance between vehicles diminishes, the air vortices trailing the leading vehicle become smaller, leading to a proportional decrease in aerodynamic drag. The reduction in aerodynamic drag leads to a decrease in fuel consumption of up to 10% for follower vehicles, according to several independent studies. Since around 25% of the fuel consumption of a heavy-duty vehicle is related to aerodynamic drag, the fuel efficiency gains can be significant. However, maintaining short inter-vehicular

distances requires precise control of longitudinal dynamics.

In addition to reducing fuel consumption and greenhouse gas emissions, platooning offers other benefits, including improved safety and more efficient use of road infrastructure. In Europe, heavy-duty vehicles are involved in 4.5% of police-reported road crashes and account for 14.2% of collisions involving severe or fatal road accidents [16]. The automation of longitudinal dynamics through platooning would result in a substantial reduction in the occurrence of such accidents. This is because the driver actions depicted in Figure 1.1 can either be eliminated entirely or executed with greater speed and efficiency. Moreover, platooning can be seen as a precursor to fully automated vehicles, which are expected to greatly reduce fatalities, especially, on the highways. Finally, the short distance between vehicles in platooning would increase the capacity of current highways without the need to construct additional lanes.

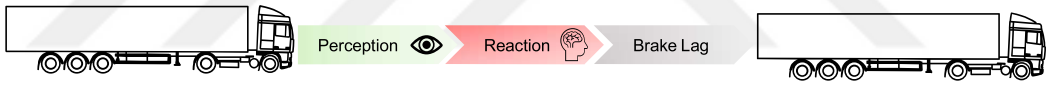

Figure 1.1. Manual driving: driver perception, reaction, and brake lag illustration.

In order to create platoons of vehicles, proper coordination is necessary. Highways generally have a relatively limited presence of heavy-duty vehicles, resulting in their sparse distribution throughout the road network. For instance, some vehicles may have to change their route or speed to approach other heavy-duty vehicles, but these actions must be planned based on fuel economy criteria. Nevertheless, accelerating to catch up with a platoon that is about to disperse can lead to higher fuel consumption compared to driving alone at a consistent average speed. Therefore, in order to establish a sustainable freight transportation system, it is crucial to address fuel efficiency concerns at multiple levels. This includes coordinating and planning vehicle routes, as well as implementing local control measures for individual vehicles and platoons.

1.1.2. Enabling Platooning Technologies

The demands on driver performance have intensified as traffic density rises and networks become more complex. Maintaining a close inter-vehicle spacing requires constant vigilance and adjustment of velocity and distance according to the lead vehicle's behavior, which is a highly demanding task for the driver. Human drivers' response time is often insufficient to maneuver the vehicle safely and efficiently under such conditions, resulting in unnecessary harsh braking, acceleration, or even accidents. Fortunately, recent technological advancements have led to the development of systems that can assist drivers in platooning applications.

In recent years, there has been a notable surge in the installation of electronic control systems and sensors in vehicles, enabling enhanced software functionality and intelligent control mechanisms. ADAS has been developed as a result, with features such as lane departure warning systems that issue a warning when a driver veers out of their lane, using a camera mounted in the front window. Furthermore, the implementation of downhill speed control aims to assist heavy-duty vehicles in sustaining optimal speeds when traversing downhill stretches. In a similar vein, the utilization of adaptive cruise control, readily accessible in the market, has been proposed as a facilitative mechanism for enabling vehicle platooning by utilizing radar or lidar technology to establish control strategies based on the distance and velocity of a preceding vehicle.

The topography of roads greatly influences how heavy-duty vehicles operate. While descending a hill, a heavy-duty vehicle gains speed without relying on the engine's power, and when ascending the next hill, it slows down despite applying maximum engine torque. To address this issue, a fuel-efficient control systems known as look-ahead control (LAC) and cooperative look-ahead control (CLAC) has been developed [17–19]. The system utilizes road map information to generate suitable control commands for the engine and gearbox control systems. This enables the vehicle to anticipate the power requirements of upcoming hilly road sections, effectively minimizing fuel consumption and reducing its environmental impact. For example, by

reducing the speed prior to approaching a downhill section, it is possible to prevent unnecessary braking and achieve a substantial reduction in overall fuel consumption. Currently, map service providers have regional constraints on providing comprehensive road grade information. Nevertheless, vehicle manufacturers can utilize their own on-board sensors and GPS system to acquire accurate road grade information.

Vehicle-to-vehicle (V2V) and vehicle-to-infrastructure (V2I) communication technologies have evolved to enable platooning, and the IEEE 802.11p communication protocol has been developed for wireless access in vehicular environments [20]. Initially designed for short-range communication in vehicle-based networks, IEEE 802.11p has been enhanced to support high-speed data exchange between vehicles and roadside infrastructure. The European Commission has licensed part of the 5.9 GHz band for road safety applications and inter-vehicle, infrastructure communications [21]. The Car 2 Car communication consortium has been dedicated to establishing a universal standard for V2X communication. Simultaneously, the European Commission has called upon major stakeholders to collaborate on creating a unified framework of standards and guidelines for cooperative intelligent transportation systems. However, before V2X information can be effectively transmitted over the mobile broadband network, it is crucial to address latency concerns, particularly for time-sensitive vehicle control applications.

Wireless communication offers a broad range of information that can be utilized to enhance control strategies, resulting in reduced fuel consumption and emissions. V2X communication can provide both local and global information, such as the behavior of vehicles within a platoon, traffic routing, and safety issues. This information can be used to develop strategies based on a broad range of events, making it possible to improve performance significantly. However, there are still several issues that need to be resolved, including standardization, safety, and economic feasibility. Therefore, implementing new technologies must be approached with care to ensure that they are suitable for widespread implementation.

1.2. Spacing Strategies in Platooning

The fundamental element of any adaptive cruise control (ACC) system or cooperative adaptive cruise control system (CACC) is the spacing policy, which determines the desired distance between two vehicles during vehicle following. This policy holds significant importance across various dimensions, including traffic capacity, safety, energy consumption, and driver acceptance. Prior research on spacing policies has primarily concentrated on managing the longitudinal control of personal rapid transit (PRT) and automated highway systems (AHS). Due to the swift advancement of adaptive cruise control systems, these studies have been successfully applied to ACC designs. In recent years, there have been numerous efforts to improve spacing policies, resulting in many fascinating findings in the literature [22]. This section explains various spacing policies by grouping them according to how they function and thoroughly examines the features of each policy.

1.2.1. Evaluation Criteria of Spacing Policies

The task of selecting a spacing policy is inherently complex, as it involves multiple design objectives that are often contradictory in nature. For example, reducing the distance between vehicles can increase traffic capacity, but it can also jeopardize safety if the gap becomes too narrow. As a result, an effective spacing policy requires striking a delicate balance between various design objectives. The spacing policies are evaluated based on certain criteria in the literature, which are explained in detail in the following section.

(i) Individual Vehicle Stability: One of these criteria is the assurance of individual vehicle stability, which is achieved by ensuring that the spacing error of the host vehicle, represented by δ_i, converges to zero if the preceding vehicle operates at a constant speed, denoted by v_{i-1}. This can be mathematically expressed as

$$\delta_i = d_i - d_{des} \qquad \dot{v}_{i-1} \to 0 \Rightarrow \delta_i \to 0, \tag{1.1}$$

where d_i is the actual inter-vehicle spacing between the $i-1$th and the ith vehicles, and d_{des} is the desired inter-vehicle spacing. The stability of each vehicle is essential for the CACC system to perform its fundamental functions.

(ii) String Stability: When selecting a spacing policy, it is important to also consider an accompanying controller that ensures the string stability of a platoon. The string stability of a platoon refers to the property that limits spacing errors from diverging as they propagate toward the tail of the platoon, and it is a group property that describes the interaction between the vehicles in the platoon. This is different from individual stability which only concerns a single vehicle. It has been suggested that the string stability of a platoon is directly related to the spacing policy selected. A more stringent requirement for string stability arises when examining the propagation of specific signals from the preceding vehicle $i-1$ to the current vehicle i. This condition is expressed in terms of the strong string stability transfer function, which is defined as in [23], as

$$S^s_{\Delta_{i,i-1}}(s) := \frac{\Delta_i(s)}{\Delta_{i-1}(s)},\ i \in \mathbb{N}_{[1,n]},\ s \in \mathbb{C}, \tag{1.2}$$

where $\Delta_i(s) := \mathcal{L}(\delta_i)$ with $\mathcal{L}$ is the Laplace operator and δ_i is the spacing error between the consecutive vehicles as well as the signal of interest to evaluate the string stability. Based on this definition, the following condition for strong string stability can be expressed as

$$\|S^s_{\Delta_{i,i-1}}(s)\|_{\mathcal{H}_\infty} \leq 1,\ \forall i \in \mathbb{N}_{[1,n]}, \tag{1.3}$$

where the left-hand side of the inequality in (1.3) stated as

$$\|S^s_{\Delta_{i,i-1}}(s)\|_{\mathcal{H}_\infty} = \sup_{w\in\mathbb{R}} \left|S^s_{\Delta_{i,i-1}}(jw)\right|. \tag{1.4}$$

(iii) Traffic Flow Stability: This overall characteristic represents the manner in which traffic flow changes in relation to slight adjustments in traffic density, assuming that all vehicles on the road adhere to the same spacing policy. In order to assess whether the system maintains traffic stability, the gradient of the traffic flow rate

with respect to the traffic density is typically used [24] as follows

$$\frac{\partial Q}{\partial \rho_t} > 0, \tag{1.5}$$

where ρ_t represents the traffic density, while Q indicates the rate of the traffic flow. However, achieving traffic flow stability for all traffic densities, regardless of the spacing policy used, is impractical [22]. Nonetheless, it is crucial to strive towards maximizing the range of traffic densities where traffic flow stability can be ensured.

(iv) Collision Avoidance: Ensuring the safety of the host vehicle is a crucial requirement for any spacing policy, aiming to prevent collisions caused by unexpected actions of the vehicle in front. This safety-focused criterion sets strict security constraints on the policy's design [25]. While criteria for individual vehicle stability and string stability also contribute to safety, they serve as necessary but not sufficient conditions for collision avoidance. Their primary focus is achieving stability performance rather than prioritizing safety, and they do not guarantee complete collision prevention. Therefore, to effectively prevent collisions when the preceding vehicle acts unpredictably, it is vital to consider this essential safety criterion in the spacing policy's design.

(v) Driving Pattern: In order to ensure a comfortable experience for the driver and passengers, it is crucial for the spacing policy to mimic the natural driving behavior.

1.2.2. Types of Spacing Policies

In the realm of ACC or CACC, spacing policies can be generally categorized as constant spacing policies and adaptive spacing policies. The subsequent discussions delve into the specific attributes and qualities of these spacing policies. To thoroughly explore the different spacing policies, a comprehensive survey is conducted in a relevant study [22].

The constant spacing policy (CSP) refers to a spacing policy in which the ACC vehicle maintains a fixed distance from the preceding vehicle throughout the operation of ACC, regardless of the driving conditions. The CSP [26, 27] can be expressed as

$$d_{des} = L, \tag{1.6}$$

where the desired inter-vehicle spacing is represented by d_{des}, while L is a fixed constant. Choosing a small value for L can improve traffic capacity, but it may compromise safety when CSP, which has a low computational load, is applied. Some studies suggest that the optimal value for L should be established as 1 meter. However, the CSP has been proven to be unable to ensure string stability when linear controllers are used, which may lead to poor ride quality and collisions. To address this issue, some studies propose maintaining continuous inter-vehicle communication to ensure string stability when implementing CSP. Once string stability is achieved, a small L can enhance traffic capacity, which is utilized in the development of CACC systems that are based on CSP. Nevertheless, ensuring reliable and high-quality inter-vehicle communication becomes increasingly challenging as platoons grow longer. This difficulty is a primary reason why no existing ACC system has adopted the CSP as mentioned in [22].

Unlike the constant spacing policy, adaptive spacing policies adjust the desired inter-vehicle spacing based on the speed of the host vehicle. In the literature, four primary categories of adaptive spacing policies are identified based on their underlying operating mechanisms. These include the time headway-based spacing policy, traffic flow stability spacing policy, constant safety factor spacing policy, and human driving behavior spacing policy. These spacing policies aim to improve the string stability of platoons and safety performance while maintaining the traffic capacity. Among these policies, the time headway-based policy stands as the most commonly utilized approach in ACC systems due to its simplicity and good performance. It determines the inter-vehicle spacing as a function of the time headway, which is the time interval between the host vehicle and the preceding vehicle. The other three types of adaptive spacing policies take into account the traffic flow stability, safety factor, and human driving behavior, respectively, and adjust the inter-vehicle spacing accordingly. These policies

have been shown to provide good performance in simulations and field tests; however, will not be discussed further in this study.

Time-Headway Based Spacing Policy is the most common type of adaptive spacing policy used in literature. Sometimes, the term "time gap" is used interchangeably with "time headway" in some studies. Nonetheless, the terms time gap and time headway have distinct quantitative meanings. The time gap refers to the duration between the rear bumper of the preceding vehicle passing a fixed point on the road and the front bumper of the host vehicle passing the same point. On the other hand, time headway represents the duration between the front bumper of the preceding vehicle passing the fixed point and the front bumper of the host vehicle passing the same point. Although there are quantitative distinctions between these two terms, they ultimately result in similar vehicle behavior when considered qualitatively. Hence, this chapter categorizes both as the time headway-based spacing policy, which can be defined by using the speed of the host vehicle, and the time headway as

$$d_{des} = \tau v_h + d_{min}, \tag{1.7}$$

where τ, v_h and d_{min} are the time headway, the host vehicle's speed, and the minimum allowed clearance, when both the preceding and host vehicles come to a complete stop, consecutively. There are two common types of time headways: constant time headway (CTH) and adaptive (or variable) time headway (ATH). In CTH, τ is a fixed value, while in ATH, it can vary.

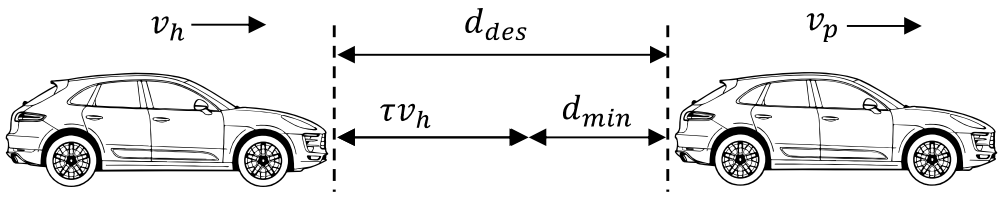

Figure 1.2. Visualization of a spacing policy based on time headway.

Alternatively, the time headway-based spacing policy can be defined by using the preceding vehicle's speed, represented by v_p, rather than relying on the speed of the

host vehicle and multiplying it with time headway stated as

$$d_{des} = \tau v_p + d_{min}. \tag{1.8}$$

Nevertheless, this approach suffers from a fundamental drawback. In situations where the trailing vehicle travels at a considerably higher speed than the leading vehicle, for example, at 70 kph compared to 40 kph, the desired spacing between the vehicles would be determined based on the lower speed of the leader. This inherent limitation greatly elevates the risk of severe collisions [28]. A graphical representation of the time headway-based spacing policy is presented in Figure 1.2.

The constant time headway (CTH) spacing policy [27, 29] maintains a fixed time gap between the preceding and host vehicles, which is proportional to the vehicle speed. This policy aligns with the driving instinct of reducing the speed as the inter-vehicle distance shrinks. The choice of time headway value significantly impacts driver perception and experience, such as perceived risk, task complexity, effort, and comfort. Empirical data from driving tests can be used to determine the appropriate values of τ and d_{min} for the CTH policy. Commercially available ACC systems usually provide a choice of τ ranging from 1s to 2s. In contrast to the CSP, the CTH spacing policy can ensure string stability without the need for inter-vehicle communication [29]. However, an excessively small τ can still compromise string stability, so the appropriate value of τ should be selected based on system requirements. CTH has gained widespread adoption and recognition as the prevailing policy in both academia and the automotive industry and it is likely to be used in future CACC systems, enabled by inter-vehicle communication technology.

On the other hand, the CTH spacing policy may not be appropriate for high-density traffic situations due to two reasons. Firstly, it increases the gap between vehicles, resulting in a decrease in traffic throughput. Secondly, it is unable to ensure traffic flow stability, as observed in several studies. To address the issue of reduced traffic throughput caused by the CTH spacing policy, the ATH spacing policy was

introduced in 1995 by Yanakiev and Kanellakopoulos [30] and can be expressed as

$$\begin{aligned} \tau &= h_0 - c_1 v_r \\ v_r &= v_p - v_h, \end{aligned} \tag{1.9}$$

where both h_0 and c_1 are positive constants. The value of time headway is always greater than zero, but it should not be too large as it may lead to reduced traffic throughput. The ATH spacing policy proposed by Yanakiev and Kanellakopoulos limits the time headway to the interval [0, 1] as expressed by the following operation

$$\tau = \begin{cases} 1 & \text{, if } h_0 - c_1 v_r \geq 1 \\ h_0 - c_1 v_r & \text{, if } 0 < h_0 - c_1 v_r < 1 \\ 0 & \text{, otherwise} \end{cases} \tag{1.10}$$

Another version of the ATH spacing policy was proposed by Broqua [31], where the time headway (τ) is a variable that depends on the host vehicle speed. This spacing policy can be mathematically represented as

$$\begin{aligned} d_{des} &= \tau v_h + d_{min} \\ \tau &= h_1 + h_2 v_h, \end{aligned} \tag{1.11}$$

where the constant values h_1 and h_2 are positive. The time headway τ in the ATH spacing policy increases with the host vehicle speed v_h and is bounded by an upper limit v_{max}. This relation can be shown as

$$\tau = \begin{cases} h_1 + h_2 v_h & \text{, if } v_h < v_{max} \\ h_1 + h_2 v_{max} & \text{, otherwise} \end{cases} \tag{1.12}$$

1.3. Motivation of the Thesis

Cooperative Adaptive Cruise Control (CACC) uses communication between vehicles to coordinate their movements and maintain a safe distance from each other. The

spacing strategies used in CACC applications can be classified into two time headway-based categories: constant and adaptive time headway strategies. In CTH, each vehicle maintains a distance from the vehicle in front, which is determined by a set time headway. The lead vehicle sets the speed, and the following vehicles automatically adjust their speed to maintain the fixed time headway. In ATH, the distance between vehicles changes dynamically based on the adjustments in time headway. The lead vehicle still sets the speed, but the following vehicles adjust their speed and distance based on the lead vehicle's behavior and the traffic conditions. Both constant and adaptive spacing strategies have their advantages and disadvantages. Constant spacing is simpler to implement and easier for drivers to understand, but it may not be as flexible in adapting to changing traffic or road conditions.

Adaptive spacing, on the other hand, has the potential to offer several benefits over the constant spacing strategy. One of the primary benefits is increased flexibility and adaptability. With variable spacing, the distance between vehicles can be adjusted based on traffic conditions, road topography conditions, or the speed of the platoon. This can help improve traffic flow, reduce congestion, and increase the capacity of the roadway. Another potential benefit of the variable spacing strategy is improved fuel efficiency. By allowing the distance between vehicles to vary based on road conditions and the speed of the platoon, CACC can help reduce the number of hard accelerations and sudden braking events, which can increase fuel consumption. Studies have shown that CACC systems using variable spacing strategies can result in a fuel consumption decrease of approximately 10% compared to traditional cruise control systems. Furthermore, CACC systems using variable spacing strategies have the potential to reduce emissions and improve air quality by reducing the number of start-stop events in traffic, which can lead to decreased emissions from idling and acceleration.

Research has shown that adaptive spacing strategies can be particularly effective at improving fuel efficiency while maintaining acceptable levels of safety and string stability. For example, the look-ahead cruise control approach for HDV platooning is tested for uphill and downhill segments of a road in [17, 18] to achieve fuel reduction.

Another work was conducted based on a linearized fuel consumption map, a linear MPC is designed for the CTH strategy in [32] and showed a noticeable decrease in fuel consumption. Moreover, a cooperative look-ahead control method based on dynamic programming is applied for safe and fuel-efficient HDV platooning in [19] under constant distance and time headway strategies. The results depict the fuel-saving effectiveness of the proposed controller. Furthermore, the effect of the adaptive time headway on the aerodynamic drag resistance and fuel consumption is investigated in [33]. Finally, the distributed nonlinear model predictive approach is applied in [34] for avoiding energy-inefficient maneuvers and improving fuel consumption based on an instantaneous fuel consumption model.

Table 1.1 provides a summary of the mentioned contributions of the relevant studies, aiming to illustrate the similarities and differences compared to the proposed method in this thesis, which is shown with the symbol (∗) in the last row of the table. The abbreviations "L" and "NL" in the "Model" column of the table stand for linear and nonlinear models, respectively to categorize the models used in the summarized work.

Table 1.1. Summary of the related studies in the literature.

Ref.	**Spacing**			**Method**			**Model**		**Focus**		
-	CSP	CTH	ATH	DP	MPC	NMPC	L	NL	Fuel	Slope	Drag
[17]			✓	✓			✓	✓	✓	✓	
[18]		✓			✓		✓		✓	✓	✓
[19]	✓	✓		✓	✓		✓	✓	✓	✓	✓
[32]		✓			✓		✓		✓		
[33]			✓	✓			✓	✓	✓	✓	✓
[34]		✓				✓	✓	✓	✓		✓
*		✓	✓			✓	✓	✓	✓	✓	✓

Although the aforementioned studies separately inspected different parts of HDV platooning, a broad investigation that brings all the key elements together is aimed in this study. Minimization of fuel consumption considering the nonlinear fuel consumption approximation and the nonlinear air drag coefficient is managed by a fuel-efficient NMPC controller that regulates an adaptive time headway strategy. Moreover, a closed-loop simulation environment is established for both homogeneous and heterogeneous platoons to apply CTH and ATH strategies generated by NMPC under different road topography conditions. This creates a comparison baseline for fuel consumption metrics of the different spacing strategies and proves the efficacy of the proposed control method.

1.4. Outline of the Thesis

This thesis is organized as follows:

Chapter 2 presents a comprehensive overview of the essential components and models employed in the platooning study. It encompasses the development of a dynamic model for the platoon, capturing the intricate dynamics of the vehicles and their interactions. Additionally, a nonlinear air drag model is introduced, accounting for the impact of time headway on aerodynamic drag. Furthermore, the chapter introduces a benchmark truck model that serves as a crucial testing ground for evaluating the effectiveness of the designed nonlinear model predictive controller (NMPC) in a closed-loop setting. This truck model enables the assessment of the controller's performance and its ability to achieve fuel efficiency goals. Additionally, the chapter delves into the fuel consumption approximation of a diesel engine, an integral component for quantifying and optimizing fuel efficiency. This approximation plays a pivotal role in the control design process, facilitating the development of fuel-efficient strategies using the model predictive controller.

Chapter 3 serves as a comprehensive guide to the essential concepts and methodologies employed in the field of Model Predictive Control, with a specific focus on its

application in platooning scenarios. The chapter lays the groundwork by providing a solid understanding of the fundamental principles and motivations behind MPC. Furthermore, the chapter explains the development of Nonlinear MPC, shedding light on the specific details on highlighting why it is the preferred control method in this work for complex systems like platooning. The advantages and benefits of using NMPC in this context are discussed in detail, showcasing its ability to handle the intricate dynamics and constraints inherent in platoon control. The chapter also explores various applications of MPC in platooning, demonstrating its versatility and effectiveness in achieving diverse control objectives such as fuel efficiency, safety, and stability. Moreover, the optimization problem construction for MPC is meticulously detailed, covering the selection of appropriate cost functions and constraints. The step-by-step explanation guides the reader through the process of designing the control strategy, ensuring that the chosen objectives are properly addressed and the system's constraints are adhered to. Finally, simulation results of the designed NMPC controller are demonstrated to showcase the correct design.

Chapter 4 serves as a comprehensive exploration of the simulation setup employed to assess the performance of the designed control system in a closed-loop configuration. The chapter meticulously details the various components and intricacies of the simulation setup, providing a comprehensive understanding of the experimental framework. The simulation setup is specifically designed to facilitate the rigorous evaluation and validation of the developed Nonlinear Model Predictive Control (NMPC) approach. By utilizing a benchmark truck model, the control system is subjected to diverse real-life scenarios and conditions, enabling a comprehensive analysis of its performance under different settings. Within this chapter, eight distinct simulation scenarios are meticulously conducted, each featuring a unique combination of spacing strategies, namely Constant Time Headway (CTH) and Adaptive Time Headway (ATH), as well as different road topography conditions, which are obtained from real map data. These carefully curated scenarios ensure a comprehensive assessment of the control system's capabilities across a wide range of real-world conditions, providing valuable insights into its effectiveness and robustness. By scrutinizing the simulation results obtained

from these diverse scenarios, the chapter offers compelling evidence of the design's success and showcases its ability to deliver promising outcomes. The detailed evaluation of each scenario provides a comprehensive understanding of the control system's performance, including its fuel efficiency, stability, and adaptability to different road conditions.

Chapter 5 marks the culmination of this thesis, bringing together the key findings and insights gained throughout the study. It serves as a pivotal chapter that encapsulates the essence of the research and provides a concise yet comprehensive summary of the thesis as a whole.

2. DYNAMIC MODELS FOR FUEL-ECONOMICAL CONTROL DESIGN AND VALIDATION

In this chapter, the mathematical models that are used to represent the platoon, air drag, benchmark truck, and fuel consumption in the context of a fuel-economical control design for heavy-duty truck platooning are described. The benchmark truck model is used to capture the dynamics of the heavy-duty truck, while the air drag model represents the resistance force due to air drag. The fuel consumption model is obtained to estimate the fuel consumption of the truck based on its dynamic behavior and the resistance forces acting on it.

The benchmark truck model is based on a multi-body system, and it takes into account the dynamics of the truck, including its main components such as engine and transmission. The air drag model utilized in this study adopts a simplified approach to represent the truck's aerodynamics. It considers the drag force as a function of key parameters such as the vehicle's velocity, frontal area, and time headway. The fuel consumption model employed is an approximate representation using a non-linear piece-wise higher degree polynomial based on a combination of the engine characteristics, vehicle dynamics, and resistance forces acting on the truck, and it provides an estimate of the fuel consumption for a given driving scenario.

The mathematical models introduced in this section serve as the foundation for constructing an adaptive spacing strategy with a fuel-efficient focus for HDV platooning. By employing a nonlinear model predictive control approach, the control design seeks to optimize fuel consumption within the platoon while ensuring the maintenance of a secure and steady inter-vehicle distance. The models are used to derive the cost functions and constraints that are used in the optimization problem solved by the designed controller. The resulting control policy is designed to coordinate the longitudinal motion of the platoon trucks while taking into account the effect of the air drag and the fuel consumption of the trucks.

2.1. Platoon Model

A platoon of vehicles can be modeled as a chain of interconnected dynamic systems, where each vehicle interacts with its preceding and succeeding vehicles. The dynamics of a platoon depend on various factors such as the inter-vehicle spacing, the vehicle mass, the aerodynamic drag, and the powertrain dynamics. The leading vehicle sets the reference velocity for the platoon, and each following vehicle maintains a desired inter-vehicle spacing and velocity relative to the preceding vehicle. In general, the dynamics of a platoon can be modeled using a set of differential equations that describe the motion of each vehicle. These equations can be coupled to account for the interaction between the vehicles in the platoon. The dynamics of a platoon are critical for designing platooning control algorithms that can achieve safety, efficiency, and comfort objectives.

In order to formulate the platooning problem, a pair of equations that defines the longitudinal dynamics is required. First, the platoon model as a 2nd order linear system is derived to contribute vehicle following objective which regulates the error

$$e = r - d \tag{2.1}$$

to zero, where r is the actual distance between two consecutive vehicles and d is the desired spacing. The dynamic equations of the two following vehicles are stated as

$$\begin{aligned} \dot{\Delta x} &= v_p - v_h \\ \dot{v}_h &= a_h, \end{aligned} \tag{2.2}$$

where v_h and a_h are the velocity and acceleration of the host (ego) vehicle and v_p is the velocity of the preceding (lead) vehicle. The intervehicular distance is given by Δx, which is greater than zero. State space form of (2.2) is expressed as

$$\frac{d}{dt}\begin{bmatrix} \Delta x \\ v_h \end{bmatrix} = \begin{bmatrix} 0 & -1 \\ 0 & 0 \end{bmatrix}\begin{bmatrix} \Delta x \\ v_h \end{bmatrix} + \begin{bmatrix} 0 \\ 1 \end{bmatrix} a + \begin{bmatrix} 1 \\ 0 \end{bmatrix} v_p, \tag{2.3}$$

where $[\Delta x\ , v]^{\mathrm{T}} \in \mathbb{R}^{2x1}$ is the state vector, a is the manipulated variable and v_p is the measured disturbance obtained via the assumed predecessor-leader following (PLF) communication topology. The string stability of the platoon, which contains 2 vehicles, is not considered as explained in Section 1.1.

2.2. Aerodynamic Drag Model

Aerodynamic drag is an important factor that affects the fuel consumption of vehicles. It is determined by the vehicle's shape and its interaction with the air. The drag force is typically modeled as a function of the vehicle's velocity, frontal area, and coefficient of drag. The resistance caused by aerodynamic drag can have a significant impact on heavy-duty vehicles, up to 50% of the total resistive forces at full speed. According to studies, one effective method to reduce wind resistance is by arranging trucks in a platoon formation.

Platooning uses the concept of drafting, also known as slipstream, which involves utilizing the airflow behind each vehicle that has not yet been disrupted. This results in the vehicles following behind experiencing lower air pressure [35]. The overall aerodynamic drag is caused by a pressure difference between the front and rear of a vehicle. While the two following vehicles are cruising close to each other, the pressure difference between the follower vehicle's front and rear is not significantly divergent. As the distance between the lead vehicle and the follower vehicle decreases, the pressure acting on the front of the follower vehicle is considerably reduced, resulting in a decrease in its aerodynamic drag [4]. Additionally, the lead vehicle gains an advantage from the close proximity of a following vehicle because the follower vehicle's influence on the wake of the first vehicle leads to a rise in pressure on the rear of the first vehicle. This results in a decrease in total air drag and subsequently reduces fuel consumption.

In platooning, the drag force is also influenced by the time headway between vehicles. The closer the vehicles are, the less air can flow between them, resulting in a reduction of the drag force. Therefore, the aerodynamic drag model that is planned

to be used in the platooning application should take into account the time headway as an additional factor that affects the overall drag force. This model allows for the optimization of the time headway to minimize fuel consumption while maintaining the safety and stability of the platoon.

In this study, the air drag coefficient is considered as a nonlinear function of time headway (τ_i) between the ego vehicle and its leading vehicle, as evaluated in [33]. In this formulation, time headway refers to the interval between two consecutive vehicles passing a specific point on the road (the distance between vehicles in time) and can be calculated as $\tau = \Delta x / v_h$ by using the states defined in (2.2). The model for the air drag coefficient can be represented as

$$C_D(\tau_i) = C_D^0 \left(1 - \frac{\alpha_1}{1 + \alpha_2 \tau_i}\right), \tag{2.4}$$

where C_D^0 represents the base air drag coefficient for a single heavy-duty vehicle operating independently, while the parameters α_1 and α_2 govern the reduction in air drag as the time headway between vehicles decreases. It is important to highlight that relationship between the air drag coefficient and time headway is crucial for the understanding of the platooning concept. As (2.4) depicts, decreasing the intervehicular distance between vehicles decreases aerodynamic forces, resulting in reduced fuel consumption [36].

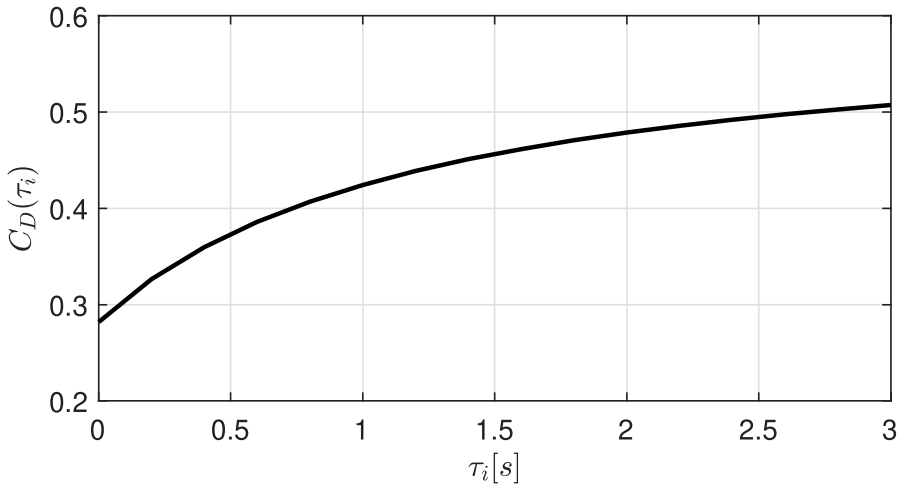

Figure 2.1. Air drag coefficient $C_{D_i}(\tau_i)$ as a function of time headway τ_i.

The nonlinear relationship defined in (2.4) can be further derived to determine the air drag coefficient of each platoon member separately as

$$C_{D_i}(\tau_i) = \begin{cases} C^0_{D_i} & \text{, if i = 0} \\ C^0_{D_i}\left(1 - \alpha_{1_i}/(1 + \alpha_{2_i}\tau_i)\right) & \text{, otherwise} \end{cases} \tag{2.5}$$

where i represents the vehicle order in the platoon. Lead vehicle ($i = 0$) is exposed to the nominal air drag coefficient ($C^0_{D_i}$) where the follower vehicles have the possibility to reduce the air drag coefficient depending on their time headway. By applying this generalized formula, it would be easier to evaluate the aerodynamic drag coefficient of each vehicle in a heterogeneous platoon in which characteristics are different; hence, the coefficients in (2.5) would be non-identical.

2.3. Benchmark Truck Model

An HDV model, originally presented as a reference problem in [37], serves as a benchmark for developing fuel-efficient control strategies for long-haul heavy-duty trucks traveling on an open road with a specified road profile, is used in this work as the heavy-duty truck plant model for verification and validation of the designed nonlinear model predictive controller (NMPC). The details of the HDV model will be given in the following subsections. The utilized truck model consists of five subsystems: Internal Combustion Engine (ICE), Clutch and Transmission, Transmission Control Unit (TCU), and Chassis as shown in Figure 2.2.

There are five possible controls inputs to the benchmark truck model as requested gear $u_{g,r}$ [-], EGR valve u_{egr} [%], VGT opening u_{vgt} [%], fuel injection u_δ [$mg/stroke$] and brake control u_b [%]. For the sake of simplicity and compactness, not all of the control inputs are generated by the designed controller. Gear request,$u_{g,r}$, is generated by the given default gear shifting logic and handled by the TCU in Figure 2.2. EGR valve, u_{egr}, and VGT opening, u_{vgr}, are given constant as 0 and 45 respectively as given default in the benchmark problem. Only u_δ and u_b are in the control focus of this

work. Additionally, the road slope is consumed by the plant model as an environmental disturbance caused by the road topography. Control design relevant outputs position, x and speed, $\dot{x}$, of the truck model are measured from the system which then feeds into the controller to determine the optimal control action.

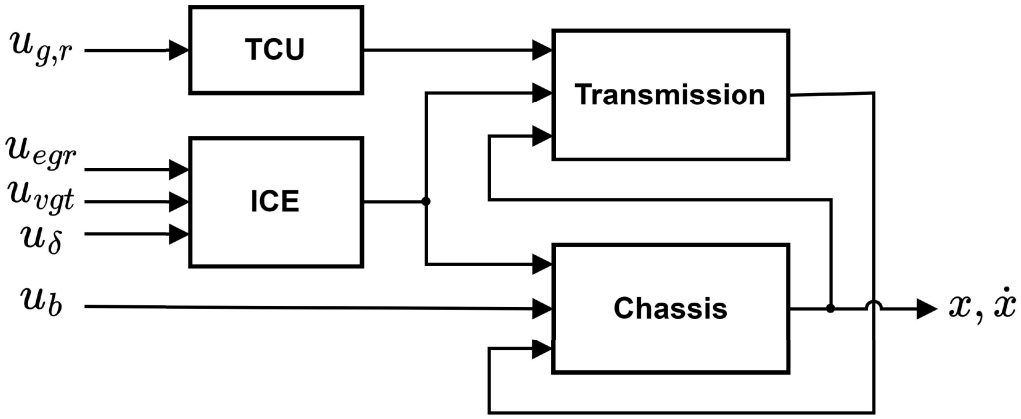

Figure 2.2. Block diagram of the benchmark heavy-duty truck model.

2.3.1. Internal Combustion Engine

The benchmark truck model (BTM) features a 12.7-liter, 6-cylinder diesel engine, equipped with an exhaust gas recirculation (EGR) system and a variable-geometry turbocharger (VGT). Figure 2.3 provides a visual representation of the engine's torque, power, and fuel consumption characteristics, as depicted in the engine catalog.

The BTM is designed to deliver performance with a maximum torque of 2110 Nm and maximum power output of 295 kW, ensuring a strong source of power for the truck by consuming injected fuel as an input for its ignition system. By utilizing the capabilities of the BTM, the research aims to explore the potential for reducing fuel consumption and optimizing efficiency in platooning scenarios. The engine's characteristics serve as a foundation for the development and evaluation of control strategies that can enhance fuel efficiency.

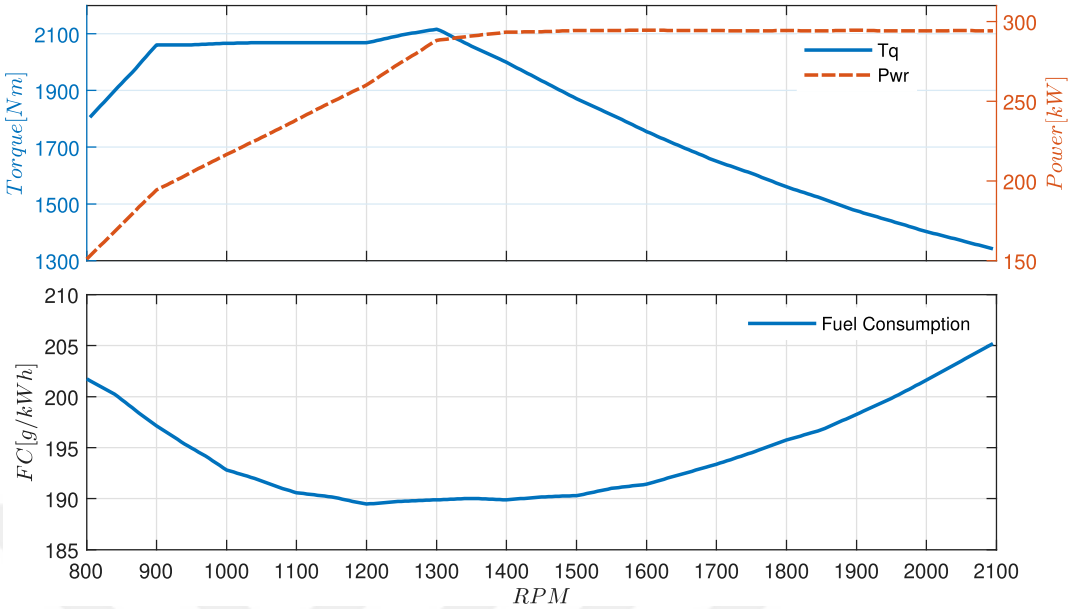

Figure 2.3. Characteristics curves of the diesel engine.

The engine model includes state variables for pressure and oxygen fraction in the intake and exhaust manifolds, which are calculated using a mass balance and isothermal model proposed by Eriksson and Nielsen [38] summarized as

$$\frac{d}{dt}p_{im} = \frac{R_a T_{im}}{V_{im}}\left(\dot{m}_c + \dot{m}_{egr} - \dot{m}_{ei}\right) \tag{2.6}$$

$$\frac{d}{dt}p_{em} = \frac{R_e T_{em}}{V_{em}}\left(\dot{m}_{eo} - \dot{m}_t - \dot{m}_{egr}\right) \tag{2.7}$$

$$\frac{d}{dt}X_{Oim} = \frac{R_a T_{im}}{p_{im} V_{im}}\left(\left(X_{Oem} - X_{Oim}\right)\dot{m}_{egr} + \left(X_{Oc} - X_{Oim}\right)\dot{m}_c\right) \tag{2.8}$$

$$\frac{d}{dt}X_{Oem} = \frac{R_e T_{em}}{p_{em} V_{em}}\left(X_{Oe} - X_{Oem}\right)\dot{m}_{eo} \tag{2.9}$$

The engine model is composed of submodels that handle different flows. It includes pressure and oxygen fraction states for intake and exhaust manifold pressures, which are calculated using the mass balance and isothermal model described in [38]. The oxygen fraction states for the intake and exhaust manifold are particularly relevant when using Exhaust Gas Recirculation (EGR), as they allow for tracking of the fresh and burned gas fractions in the system. Finally, the fifth state is the turboshaft speed,

ω_t, which is derived from Newton's second law as follows

$$\frac{d}{dt}\omega_t = \frac{\dot{W}_t\eta_m - \dot{W}_c}{J_{tc}\omega_t}, \tag{2.10}$$

where J_{tc} represents turbo inertia, $\dot{W}_t$ is the power generated by the turbine, $\dot{W}_c$ is the power needed to run the compressor, and η_m is the mechanical efficiency of the turbocharger.

Volumetric efficiency η_{vol} based total mass flow $\dot{m}_{ei}$, which is between the intake manifold and cylinders, is modeled as

$$\dot{m}_{ei} = \frac{\eta_{vol}\left(p_{im}, N\right) p_{im} N V_d}{120 R_a T_{im}}, \tag{2.11}$$

where p_{im} is the pressure and T_{im} is the temperature of the intake manifold, N and V_d are the engine speed and displacement volume respectively. The model for volumetric efficiency is expressed as a nonlinear function of intake manifold pressure and engine speed, which is presented as

$$\eta_{vol}\left(p_{im}, N\right) = c_{vol_1}\sqrt{p_{im}} + c_{vol_2}\sqrt{N} + c_{vol_3}. \tag{2.12}$$

The relation between the injected fuel and fuel mass flow is defined as

$$\dot{m}_f = \frac{10^{-6}}{120} u_\delta N n_{cyl}, \tag{2.13}$$

where N is the engine speed and n_{cyl} is the number cylinders. The fuel mass flow $\dot{m}_f$ into the cylinders is controlled by u_δ, which gives the injected mass of fuel in mg per cycle and cylinder. Equation (2.13) is crucial since the main propulsion source of the BTM can only be controlled by the injected fuel. This phenomenon is used to establish an interface between the designed NMPC and the BTM. The mass flow rate out from the cylinder is determined by the mass balance equation as

$$\dot{m}_{eo} = \dot{m}_f + \dot{m}_{ei}. \tag{2.14}$$

The ratio of oxygen to fuel in the cylinder, λ_O, is expressed as

$$\lambda_O = \frac{\dot{m}_{ei} X_{Oim}}{\dot{m}_f \left(O/F\right)_s}. \tag{2.15}$$

The stoichiometric relationship between the masses of oxygen and fuel is denoted by $(O/F)_s$. The ratio of oxygen to fuel and the normalized air-fuel ratio (λ) are equivalent to each other. This ratio is a crucial limitation for the control system to prevent the generation of smoke in the benchmark.

2.3.2. Transmission with Clutch

The transmission model is based on an ideal transmission with a stiff driveline and friction clutch between the two rotating systems. This setup enables the engine to interact with the vehicle in a way that allows them to rotate independently during a clutch slip or decoupling, or to be locked together during clutch lock-up. The clutch incorporates states for the angular velocities of the engine and the wheel. On the other hand, the gearbox and final drive are modeled as rigid, frictionless, and massless elements that are combined into a single set of gears. The cogwheels in the transmission system change the torque and rotational speed. The gear ratio i_g connects the incoming and outgoing rotational velocities and torques. The clutch is responsible for transferring the torque produced by the engine as long as it is engaged. The relation between the rotational speed and torque on the two different sides of the clutch is described as

$$i_g = \omega_e/\omega_w = M_w/M_e, \tag{2.16}$$

where ω is the rotational speed and M represents torque. w and e indicate the wheel and engine sides respectively. The inertia of the gear connected to the wheel side can be effectively transferred to equivalent inertia on the clutch side through a process known as inertia matching which expressed as

$$I_v = I_w/i_g^2. \tag{2.17}$$

In the system, the position of the clutch is linked to the clutch discs which generate a force that brings the clutch discs together, called $F_c(u_{cl})$. The variable $u_{cl}(t)$ has a range of [0,1], where 0 indicates that the clutch is separated and 1 means that the clutch discs are fully pressed together. The force, $F_c(u_{cl})$, affects the maximum torque that the clutch can transfer, $M_{c,k}\left(F_c(u_{cl}(t))\right)$. To model this system, a linear model with input, u_{cl}, is used as

$$M_{c,k}\left(F_c(u_{cl}(t))\right) = M_{max,k}u_{cl}(t). \tag{2.18}$$

The Equation (2.18) models the clutch torque when the clutch disks are slipping, also known as kinetic friction. However, when the clutch is fully engaged, it can transfer a higher torque. A constant value is used to model the ratio between static and dynamic friction, which can be expressed together with the maximum static friction torque as

$$\frac{M_{c,s}(t)}{M_{c,k}(t)} = c_{s,k} \geq 1 \tag{2.19}$$

$$M_{c,s}\left(F_c(u_c(t))\right) = M_{max,k}c_{s,k}u_{cl}(t), \tag{2.20}$$

where $c_{s,k}$ is chosen as constant 1 in the model. The clutch system can be divided into two parts that require handling as Clutch Slip and Clutch Lock.

- Clutch Slip: The system includes two rotating masses operating independently in terms of speed but are linked through the transferred clutch torque. As a result, the system has two degrees of freedom within the clutch's surroundings, and the equations that determine their rotations are given by

$$J_e\frac{d\omega_e}{dt} = M_e - M_c, \tag{2.21}$$

$$J_v\frac{d\omega_v}{dt} = M_c - M_v. \tag{2.22}$$

The torque that passes through the clutch while slipping can be expressed as

$$M_{c,s} = M_{c,k}\left(F_c(u_{cl})\right) sgn(\omega_e - \omega_v), \tag{2.23}$$

where *sgn* is the signum function. Both (2.21) and (2.23) are valid as long as rotational speeds are different on the opposite sides ($\omega_e \neq \omega_v$).

- Clutch Lock: When the clutch disc connects the two rotating systems, the masses rotate at the same speed. As a result, the two surrounding masses have only one degree of freedom, and the governing equations which define their rotation behaviors are

$$(J_e + J_v)\frac{d\omega_e}{dt} = M_e - M_v, \tag{2.24}$$

$$\omega_v = \omega_e. \tag{2.25}$$

The amount of torque transferred in the clutch, $M_{c,l}$, when it is locked is influenced by the applied torques and the inertias. The transferred torque is obtained by subtracting the inertia effect of the first mass from the driving torque as

$$M_{c,l} = M_e - J_e\frac{d\omega_e}{dt}. \tag{2.26}$$

Substituting the Equation (2.24) into (2.26) gives the clutch torque as

$$M_{c,l} = \frac{M_e J_v + M_v J_e}{J_e + J_v}. \tag{2.27}$$

To determine when the clutch breakup occurs, the transferred torque from the locked clutch, $M_{c,l}$, is compared with the maximum static friction as described in (2.20). The implemented Simulink model simulates the system using the two-state system (2.21) with two versions of the clutch transmitted torque, depending on whether the clutch is slipping (2.23) or locked (2.27).

2.3.3. Transmission Control Unit

The transmission control unit (TCU) performs gear shifting once it is requested by either driver or some other controller. Following events are taking place during the gear shifting, which takes about 2 seconds and is illustrated in Figure 2.4. The clutch and engine torques are ramped down from the demanded value to zero as soon as the

shift command is received. Then, speed synchronization is handled. Lastly, the clutch and engine torques are ramped up to the desired set point. In the TCU model, speed synchronization is neglected; hence, injected fuel is cut-off during the whole transition period.

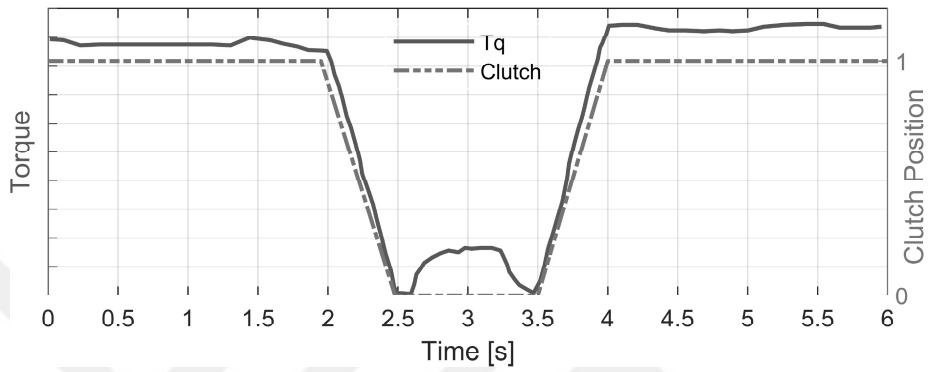

Figure 2.4. Gear change process based on clutch position and delivered torque.

2.3.4. Chassis

The chassis part contains the longitudinal vehicle model. The vehicle velocity is calculated directly from wheel speed and wheel radius relation as $v = \omega_w r_w$. The dynamic equations of vehicle motion along the longitudinal direction can be summarized by using Newton's second law as

$$\begin{aligned} m\dot{v} &= F_t - (F_b + F_a + F_r + F_g) \\ \dot{x} &= v, \end{aligned} \tag{2.28}$$

where v and x denote the speed and longitudinal position of the vehicle. m is the vehicle mass and F_t (tractive force), F_b (brake force), F_a (aerodynamic drag), F_r (rolling resistance), and F_g (gravitational force) are the forces acting on the vehicle. Figure 2.5 illustrates the longitudinal forces acting on a heavy-duty vehicle.

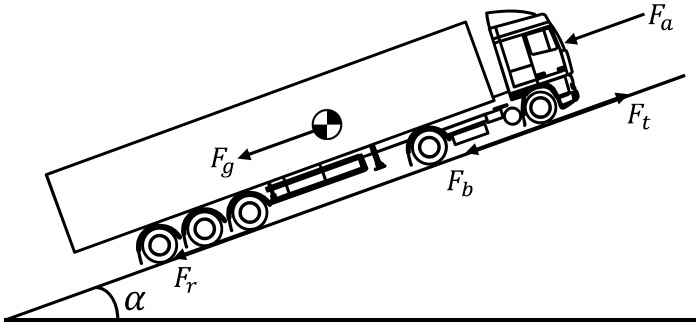

Figure 2.5. Longitudinal forces acting on an HDV.

The braking mechanism of a heavy-duty vehicle comprises multiple actuators. The braking force is regarded as a control input, and a low-level controller monitors the corresponding acceleration. The maximum torque that can be generated by the braking actuators on each axle is denoted by $T_{a,max}$. This torque is transmitted to the road surface via the tires and the wheels. As a result, the potential braking force can be calculated based on the number of axles, n_a, and wheel radius, r_w, as $-T_{a,max} n_a r_w$. However, due to the restricted friction between the road surface and the tires, a minimum threshold for the transferred braking force exists. If we assume that the vehicle mass is uniformly distributed on all axles, then we can approximate this threshold as $-\mu m g$, where μ is the positive friction coefficient of the road and g denotes the gravitational acceleration, respectively. Thus, depending on the vehicle's mass, the ability to generate the minimum braking force is constrained by either the maximum torque capacity of the braking actuators or the minimum force that can be transferred from the wheels to the ground. This restriction can be formulated by

$$max\left(-T_{a,max} n_a r_w, -\mu m g\right) \leq F_b \leq 0. \tag{2.29}$$

The gravitational force affecting the heavy-duty vehicle is represented by the longitudinal component of the gravity vector. Depending on the slope of the road, this force can either act as resistance or provide assistance to the vehicle which is given as

$$F_g(x) = m\, g\, sin(\alpha(x)). \tag{2.30}$$

Because of the considerable mass of these vehicles, even a small road inclination can generate a huge amount of gravitational force. Hence, heavy-duty vehicles face dif-

ficulties in sustaining a consistent velocity when traveling uphill or downhill, as it requires careful management to avoid surpassing the limits of engine power or relying excessively on braking.

Rolling resistance is a force that opposes the motion of a vehicle which is caused by the friction between the tires and the road surfaces. It is mainly caused by the asymmetric deformation of the tires during compression and expansion and is proportional to the vertical load on the tires. It is expressed as

$$F_r(x, v) = m\, g\, cos(\alpha(x))\, (f_0 + f_s v), \tag{2.31}$$

where f_0 and f_s represent the rolling resistance coefficient. Several factors, including tire width, pressure, and temperature can influence the magnitude of rolling resistance.

The aerodynamic drag represents a force that acts against the motion of a vehicle as a result of its interaction with the surrounding air. Its magnitude increases quadratically with the vehicle speed and can be mathematically modeled as a function of the vehicle speed and other relevant parameters as follows

$$F_a(v) = \frac{1}{2}\, C_D\, \rho\, A_f\, v^2, \tag{2.32}$$

where C_D is a constant aerodynamic drag coefficient, ρ is the air density, A_f is the cross-sectional area of the vehicle and v is the vehicle speed. Conversely, when driving in close proximity to a preceding vehicle, this opposing force can be diminished. The decrease in resistance occurs due to a slipstream effect, which creates a zone of lower pressure in front of the follower vehicle and reduces air turbulence behind the lead vehicle. The aerodynamic drag reduction is more significant for follower vehicles, and this effect is exploited by race bikers, migratory birds, and heavy-duty vehicle platooning. The aerodynamic drag model (2.32) of the host (follower) vehicle in a platoon is adjusted such that it takes into account the influence of headway time on the aerodynamic force

as stated with (2.4) in Section 2.2. This adjustment is formulated as

$$F_a(v, \tau_i) = \frac{1}{2} C_D(\tau_i)\, \rho\, A_f\, v^2. \tag{2.33}$$

The parameter values used in Equations (2.29)-(2.33) are given in Table 2.1. All vehicle parameters summarized in Table 2.1 are taken over from the referenced benchmark model given in [37] as it is claimed by the authors that they were validated by using real driving data. Wheel torque can also be obtained through the following linear relation, in which r_w is the tire radius in meters, as

$$M_w = (F_t - F_b - F_a - F_r - F_g) r_w, \tag{2.34}$$

where r_w is the tire radius in meters.

Table 2.1. Parameters for longitudinal dynamics.

Parameter	**Symbol**	**Value**	**Unit**
Air Drag Coefficient	C_D^0	0.5	-
Air Density	ρ	1.29	kg/m^3
Frontal Area	A_f	10	m^2
Tire Radius	r_w	0.5	m
Rolling Coefficient 1	f_0	0.006	-
Rolling Coefficient 2	f_s	2.3x10^{-7}	-

2.4. Fuel Consumption Model

The fuel consumption model for a heavy-duty vehicle is typically based on a combination of physical principles and empirical data. The model may consider the vehicle's weight, speed, and grade of the road to estimate the power required to maintain the desired velocity. The power requirement, in turn, is used to estimate the fuel consumption based on the vehicle's fuel efficiency, which might be influenced by various elements, including the type of engine, transmission type, and auxiliary loads. To

simplify the fuel consumption model, researchers and engineers may use empirical data to develop approximations based on factors such as vehicle speed, engine load, and gear selection. These approximations can be useful for estimating the fuel consumption of a vehicle without requiring detailed knowledge of the vehicle's specific configuration. Overall, the fuel consumption model for heavy-duty vehicles is an important tool for evaluating the efficiency of these vehicles and for developing new technologies and control algorithms to improve fuel economy and reduce emissions [39]. While the models can be complex, approximations based on empirical data can provide a useful and practical way to estimate fuel consumption in a variety of scenarios.

The fuel consumption of a vehicle at any given moment is determined by the torque and rotational speed of the engine. This study uses a diesel truck engine with an engine size of 12.7 L, whose characteristics curves are shown in Figure 2.3. This engine model is inherent to the benchmark model explained in Section 2.3. To compute fuel-efficient driving, a differentiable function for estimating fuel consumption is needed. This requires obtaining fuel consumption data f_V [ml/s] for various sampled values of velocity (ranging from 0 to 100 kph) and acceleration (from 0 to 3.0 m/s^2). A sufficient amount of data is collected from the benchmark model to have the estimation model of its fuel consumption rate. The instantaneous fuel consumption model based on vehicle speed and acceleration given in [40] is used for this purpose.

The fuel consumption estimation function is divided into two parts. The first one is for cruising with a constant speed or zero acceleration which is expressed by a 3rd-degree polynomial, where coefficients of the polynomial are approximated by a curve-fitting process, as

$$f_{cruise} = b_0 + b_1 v + b_2 v^2 + b_3 v^3. \tag{2.35}$$

Extra fuel consumption under positive acceleration is the second part of the estimation function which can be calculated as

$$f_{accel} = \hat{a}(c_0 + c_1 v + c_2 v^2). \tag{2.36}$$

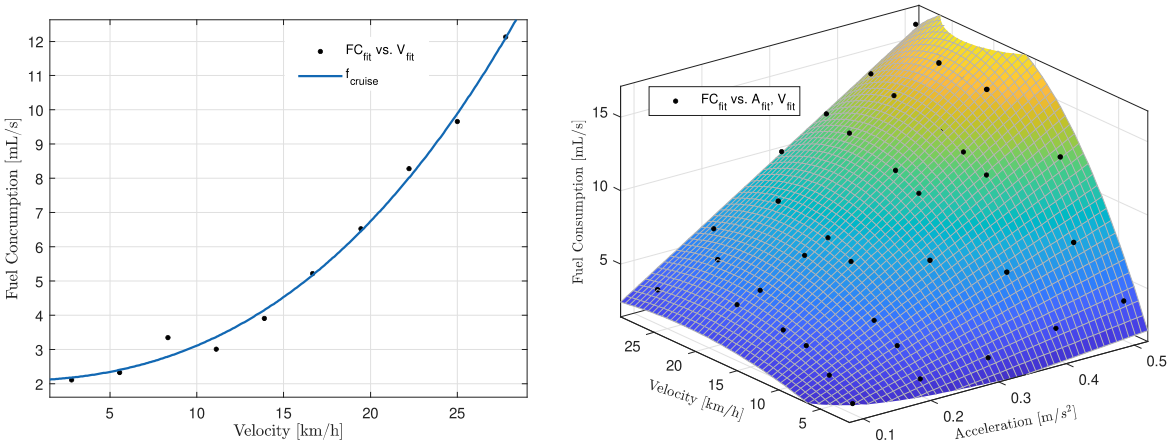

(a) Curve fitting results of f_{crs}.

(b) Curve fitting results of f_{accel}.

Figure 2.6. Curve fitting results of fuel consumption approximation.

A similar curve-fitting approach is applied to obtain the coefficients in (2.36). Here, $\hat{a}$ is the sum of the vehicle's acceleration to overcome the resistive forces and the decelerating force caused by the road gradient. By combining (2.35) and (2.36), the fuel consumption of the vehicle at any velocity and acceleration can be described by

$$f_v = b_0 + b_1 v + b_2 v^2 + b_3 v^3 + \hat{a}(c_0 + c_1 v + c_2 v^2). \tag{2.37}$$

It is assumed that if $\hat{a} < 0$, no fuel is consumed in the engine. The parameters in (2.35) and (2.36), which are obtained by the curve fitting process, are $b_0 = 0.009084$, $b_1 = -0.0002945$, $b_2 = 4.647 \times 10^{-6}$, $b_3 = -1.439 \times 10^{-8}$, $c_0 = -0.0005218$, $c_1 = 0.0007258$ and $c_2 = -1.219 \times 10^{-6}$. These parameters are substituted into (2.37) to estimate the consumption and then compared with the fuel consumption of the benchmark model for validation.

3. CONTROL PROBLEM FORMULATION

In this chapter, we will discuss how we approach the control problem. We will start by giving a brief introduction to model predictive control (MPC) and its mathematical notation. This will help us lay the foundation for our further exploration.

Next, we will focus on how MPC is used in platooning situations, where vehicles travel closely together in a coordinated manner. We will review existing studies to gain insights from their experiences. This will help us understand different methods, their strengths, and limitations. Based on this review, we will explain why we have chosen nonlinear model predictive control as the best solution for our study.

After that, we will explain the optimization problem and how it relates to our control design. We will specifically focus on nonlinear model predictive control and its design process. We want to show how this approach can effectively address the challenges and requirements of our specific problem.

Lastly, we will demonstrate how our control design meets our objectives and satisfies our needs in this particular situation. Our goal is to provide a clear understanding of the control problem formulation and highlight the practical application of our chosen approach.

3.1. Model Predictive Control

Model predictive control (MPC) is a widely adopted advanced control approach, also known as moving horizon control or receding horizon control. The primary concept behind MPC is to anticipate the future behavior of the controlled system over a defined time horizon and determine an optimal control input that satisfies given system constraints while minimizing a pre-defined cost function. To accomplish this, at every sampling time, the control input is calculated by solving a finite horizon open-

loop optimal control problem. The initial section of the optimal input trajectory is then enforced on the system until the following sampling instant, where the horizon is shifted and the process is repeated. The unique aspect of MPC is its ability to include hard input and state constraints as well as a suitable performance criterion into the controller design. This property has contributed significantly to the popularity and efficacy of MPC.

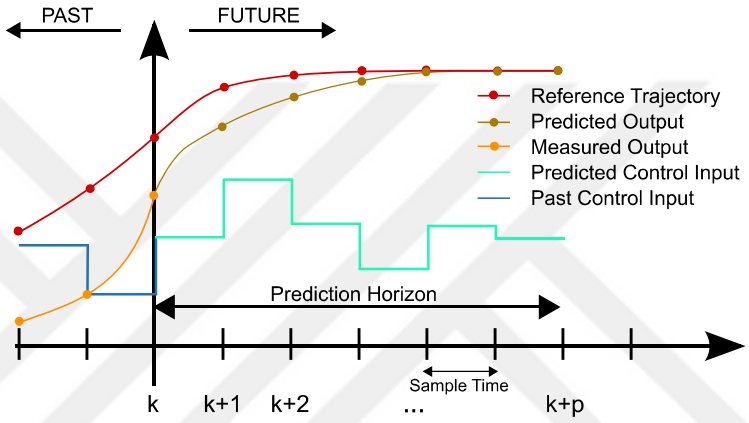

Figure 3.1. A discrete MPC scheme.

In real-world applications, MPC often retains some of the advantageous features of traditional optimal control methods, despite having a finite horizon. MPC can effectively handle MIMO plants, deal with time delays (even in different channels), and has built-in robustness to modeling errors. Additionally, by using specific terminal constraints, nominal stability can be guaranteed. MPC's capability to handle constraints and its ability to utilize information on future reference and disturbance signals (when available) are other significant features.

3.1.1. Mathematical Representation of MPC

A model predictive control where the finite time optimal control law is computed by solving an optimization problem online is also referred to as a receding horizon controller (RHC). Consider the problem of regulating to the origin the discrete-time

linear time-invariant system

$$x(t+1) = Ax(t) + Bu(t), \tag{3.1}$$

where $x(t) \in \mathbb{R}^n$, $u(t) \in \mathbb{R}^m$ are the state and input vectors, respectively. This system is subjected to the constraints

$$x(t) \in \mathcal{X},\ u(t) \in \mathcal{U},\ \forall \geq 0, \tag{3.2}$$

where $\mathcal{X} \subseteq \mathbb{R}^n$ and $\mathcal{U} \subseteq \mathbb{R}^m$ the sets are polyhedra. To address such a constrained regulation problem, Receding Horizon Control (RHC) employs the following approach. Assuming a complete measurement or estimation of the state $x(t)$ is accessible at the present time t, the finite time optimal control problem, explained in [41], can be defined as

$$\begin{aligned} J_t^*(x(t)) = \min_{U_{t\to t+N|t}} \quad & J(x(t), U_{t\to t+N|t}) = p(x_{t+N|t}) + \sum_{k=1}^{N-1} q(x_{t+k|t}, u_{t+k|t}) \\ \text{subj. to} \quad & x_{t+k|t} = Ax_{t+k|t} + Bu_{t+k|t},\ k = 0, ..., N-1 \\ & x_{t+k|t} \in \mathcal{X},\ u_{t+k|t} \in \mathcal{U},\ k = 0, ..., N-1 \\ & x_{t+N|t} \in \mathcal{X}_f \\ & x_{t|t} = x(t) \end{aligned} \tag{3.3}$$

is solved at time t, where $U_{t\to t+N|t} = \{u_{t|t}, ..., u_{t+N-1|t}\}$ and where $x_{t+k|t}$ denotes the state vector at time $t+k$ predicted at time t obtained by starting from the current state $x_{t|t} = x(t)$ and applying to the system model

$$x_{t+k+1|t} = Ax_{t+k|t} + Bu_{t+k|t} \tag{3.4}$$

the input sequence $u_{t|t}, ..., u_{t+k-1|t}$. The symbol $x_{t+k|t}$ is often interpreted as "the state x at time $t+k$ predicted at time t. Similarly, $u_{t+k|t}$ is understood as "the input u at time $t+k$ computed at time t. For example, $x_{3|1}$ represents the predicted state at time 3 when the prediction is made at time $t = 1$, starting from the current state $x(1)$. It should be noted that $x_{3|1}$ is generally distinct from $x_{3|2}$, which is the predicted state at time 3 when the prediction is made at time $t = 2$, starting from the current state $x(2)$.

Let $U^*_{t\to t+N|t} = \{u^*_{t|t}, ..., u^*_{t+N-1|t}\}$ be the optimal solution of (3.3) at time t and $J^*_t(x(t))$ the corresponding value function. Then, the first element of $U^*_{t\to t+N|t}$ is applied to system, which is given in (3.1), as

$$u(t) = u^*_{t|t}(x(t)). \tag{3.5}$$

The optimization problem (3.3) is repeated at time $t+1$, based on the new state $x_{t+1|t+1} = x(t+1)$, yielding a moving or receding horizon control strategy.

Let $f_t : \mathbb{R}^n \to \mathbb{R}^m$ denote the receding horizon control law that associates the optimal input $u^*_{t|t}$ to the current state $x(t)$, $f_t(x(t)) = u^*_{t|t}(x(t))$. Then the closed-loop system obtained by controlling (3.1) with the RHC (3.3)-(3.5) is

$$x(k+1) = Ax(k) + Bf_k(x(k)) = f_{cl}(x(k), k), k \geq 0. \tag{3.6}$$

3.1.2. MPC in Platooning Applications

Various types of controllers have been explored for longitudinal control of autonomous or semi-autonomous vehicles, each having its benefits and limitations. One widely used controller is the Proportional Integral Derivative (PID) controller, which is relatively simple to implement and compute. This controller mainly uses the distance error as the input signal, with double derivative action typically used to respond to changes in velocity and acceleration between vehicles. Studies have shown that a PD controller can be designed to be string and asymptotically stable [42]. However, the main disadvantages of PID control are that it is not an optimal control method and it cannot handle constraints, such as maintaining a minimum safety distance. To address this issue, researchers have integrated a PID controller with a reference governor, which adjusts the received reference signal from the leading vehicle to prevent any potential violation of the output constraint.

In contrast to PID control, Model Predictive Control (MPC) can incorporate constraints and optimize control sequences while satisfying them, which results in safer

platoons. With recent advancements in computational power, MPC has gained popularity in platooning research. Numerous studies have investigated the challenges of using MPC in platooning and have proposed solutions to overcome them [43]. MPC can be proven to be asymptotically stable under nominal conditions, where a quadratic cost function is used and its minimum is within the constraints sets if suitable weights are chosen. However, in practical situations, nominal conditions may not always be maintained. Hence, researchers have explored different approaches to traditional MPC to address specific limitations.

Ensuring string stability in distributed control architectures can be a challenge. A study [44] proposed a solution to this problem by introducing string stability through the use of constraints in distributed model predictive control. However, this method requires extensive vehicle-to-vehicle (V2V) communication and that the controller knows the intended trajectory of the preceding vehicle. In contrast, [45] adopted a control matching approach to tuning the weighting matrices of the MPC, which ensures that the behavior of the MPC aligns with a string-stable linear controller when the constraints are inactive. Irrespective of the intricacy of the model, the intricacy of the MPC algorithm can be adjusted by modifying either the prediction horizon or the update frequency. If the update frequency is reduced, more time can be allocated to solving the optimization problem, but this also means that the response time is lengthened. In [46], it is demonstrated that a safe update frequency is determined by the delay in the system as well as the chosen inter-vehicular distance.

MPC requires the optimization algorithm to run at each time step, which can be computationally expensive. To mitigate this issue, researchers have explored various methods to reduce the complexity of the optimization problem. The vehicle model and constraints chosen for the problem play a vital role in determining the type of optimization that should be used. The most important factor in reducing computational power is the type of optimization problem, such as linear, nonlinear, quadratic, convex, or non-convex. If the model is affine, the resulting problem can be formulated into a convex form, which simplifies the optimization process. However, oversimplification of

the model may lead to inaccurate predictions or even instability. That is why nonlinear model predictive control stands, in the literature, as a promising solution for addressing complex control problems while maintaining accurate and reliable performance. By leveraging the capabilities of nonlinear model predictive control, researchers have successfully tackled challenging scenarios, as evidenced in applications such as truck platooning [34, 47]. This approach ensures that the control system remains robust and effective without compromising the necessary complexity of the problem at hand.

3.1.3. Nonlinear Model Predictive Control

Nonlinear Model Predictive Control, NMPC, is a useful method for controlling highly nonlinear systems, especially when linear or other approaches are not applicable. It can also handle nonlinear constraints or non-quadratic cost functions. However, NMPC requires more computation power and needs a nonlinear state estimator if the full plant state is not available.

NMPC, like traditional linear MPC, calculates control actions at each control interval using model-based prediction and constrained optimization. However, NMPC differs in several key ways:

- The prediction model can be nonlinear and have time-varying parameters.
- The equality and inequality constraints can be nonlinear.
- The scalar cost function can be a nonquadratic (linear or nonlinear) function of the decision variables.

NMPC can be used to simulate closed-loop control of nonlinear plants under nonlinear costs and constraints or plan optimal trajectories by solving an open-loop constrained nonlinear optimization problem.

NMPC is the preferred control method in this study due to its suitability for addressing the defined problem (discussed in Section 3.2.1). Firstly, the problem involves

highly nonlinear models for both aerodynamic drag and fuel consumption, which are integrated into the optimization problem solved by NMPC. This makes NMPC well-equipped to handle nonlinearity effectively. Secondly, considering the nature of the problem, the expected gains from the proposed control method may not be excessively high. Therefore, simplifying the models for linear MPC implementation could result in a loss of achievable benefits. To design and simulate the NMPC controller, we utilize the Optimization Toolbox™ software in conjunction with MATLAB/Simulink™, developed by MathWorks™. This comprehensive toolbox employs the $fmincon$ function with the SQP algorithm to solve the nonlinear programming problems encountered in the NMPC controller.

3.2. Optimization Problem Formulation

In a platoon, one of the key considerations is the adjustment of the intervehicular distance between vehicles, which allows for different spacing strategies to be implemented. In this study, the focus will be on an adaptive spacing strategy that dynamically adjusts the time headway between the vehicles, based on the concept introduced in [32]. The objective is to enable the host vehicle to efficiently adapt its time headway to the lead vehicle while maintaining it within a predefined time band.

To calculate the typical intervehicular distance, we can use the equation

$$\Delta x_{des} = \Delta x_0 + \tau v, \tag{3.7}$$

where Δx_0 represents the stationary intervehicular distance, τ is the time headway, and v is the vehicle velocity. However, to ensure safety, we modify the equation by introducing a minimum level as

$$\Delta x \geq \Delta x_0 + \tau_{min} v, \tag{3.8}$$

where τ_{min} represents the minimum time headway limit before compromising the vehicle's safety. By defining this minimum constraint, we establish a lower bound on the

intervehicular distance.

On the other hand, if only fuel consumption were considered, the intervehicular distance would be larger, potentially diminishing the advantages of platooning. To prevent deviation from the desired platooning formation and to maintain traffic capacity, an upper bound needs to be defined. This maximum level can be expressed as

$$\Delta x \leq \Delta x_0 + \tau_{max} v, \tag{3.9}$$

where τ_{max} is the maximum time headway limit before breaking the platoon's formation. By defining both the minimum and maximum constraints (equations (3.8) and (3.9)), we establish an envelope within which the time headway can be adjusted efficiently.

In addition to the spacing-based constraints, it is important to consider the physical limitations of the system to ensure feasible control actions. Thus, constraints related to the vehicle's capabilities are introduced. These include minimum and maximum accelerations as a function of vehicle speed, as well as minimum and maximum vehicle speeds. Mathematically, these constraints can be expressed as

$$a_{min}(v) \leq a \leq a_{max}(v) \tag{3.10}$$

$$v_{min} \leq a \leq v_{max}, \tag{3.11}$$

where (3.10), $a_{min}(v)$ and $a_{max}(v)$ represent the minimum and maximum accelerations achievable at a given vehicle speed v. Equation (3.11) defines the range of allowable vehicle speeds, with v_{min} and v_{max} denoting the minimum and maximum values, respectively.

By considering these spacing-based and vehicle-related constraints, we establish a comprehensive problem formulation that guides the design of the platooning control system and ensures the feasibility of the resulting control actions.

Figure 3.2. Platooning scenario schematic with two trucks.

3.2.1. Nonlinear Model Predictive Controller Design

The combination of all necessary criteria, including the dynamics given in (2.2) and fuel consumption (2.37) minimization, results in a nonlinear optimization problem over a prediction horizon T subject to nonlinear inequality constraints and the initial conditions that are formulated as

$$\min_{a(t)} \int_{t}^{t+T} J\left(x(t), u(t), w(t)\right)\, dt \tag{3.12a}$$

$$\text{s.t.} \quad \Delta\dot{x}(t) = v_p(t) - v_h(t) \tag{3.12b}$$

$$\dot{v}(t) = a(t). \tag{3.12c}$$

Minimization problem and the equality constraints, which are the dynamics given in (2.2), are summarized in (3.12a)-(3.12c). Following inequality constraints complete the problem.

$$\Delta x_0 + \tau_{min} v(t) \leq \Delta x(t) \leq \Delta x_0 + \tau_{max} v(t) \tag{3.13}$$

$$a_{min}(v(t)) \leq a(t) \leq a_{max}(v(t)) \tag{3.14}$$

$$v_{min}(t) \leq v(t) \leq v_{max}(t) \tag{3.15}$$

Constraint (3.13) is related to the time headway envelope to provide the host vehicle with adaptivity. Constraints (3.14) and (3.15) are derived in order to take into account the physical vehicle limitations.

The given cost function J in (3.12a) has the following form and is the combination of six different cost terms and the related constant weights w_1, w_2, w_3, w_4, w_5 and w_6.

$$J = w_1 J_1 + w_2 J_2 + w_3 J_3 + w_4 J_4 + w_5 J_5 + w_6 J_6 \tag{3.16}$$

$$J_1 = (b_0 + b_1 v + b_2 v^2 + b_3 v^3)/v \tag{3.17}$$

$$J_2 = C_D^0 \left(1 - \alpha_1/(1 + \alpha_2 \Delta_x/v)\right) \tag{3.18}$$

$$J_3 = \frac{1}{2}\left(a + gsin(\theta(x))\right)^2 \tag{3.19}$$

$$J_4 = \frac{1}{2}(\Delta x_r - \Delta x)^2 \tag{3.20}$$

$$J_5 = \frac{1}{2}(v_p - v)^2 \tag{3.21}$$

$$J_6 = \frac{1}{2}(a_r - a)^2 \tag{3.22}$$

The first term corresponds to the fuel consumption rate (in mL/s) while cruising. Instead of solely focusing on the total consumed fuel, the aim is to optimize the fuel efficiency per distance traveled. This rate, denoted as f_V/v, is calculated using equation (2.37) with the acceleration ($\hat{a}$) set to zero. The second term accounts for the effect of the aerodynamic drag coefficient, which varies with the time headway and accounts for the impact of vehicle spacing on aerodynamic resistance. The third cost term captures the influence of acceleration forces on the vehicle, while also considering the opposing gravitational force caused by the road slope. The fourth term represents the reference tracking error of the intervehicular distance, which is calculated based on the adaptive time headway. It ensures that the desired spacing between vehicles is maintained. The fifth term represents the cost associated with not matching the velocity of the lead vehicle. This encourages the following vehicle to closely track the speed of the lead vehicle. Lastly, the sixth term accounts for the deviation of vehicle acceleration from the desired acceleration. It penalizes any deviations from the target acceleration profile. The weights assigned to each term are carefully selected to achieve a balanced trade-off between the different cost components. These weights are fine-tuned through an iterative process of observing simulation results, aiming to attain the highest possible level of fuel efficiency.

The control-oriented model that NMPC utilizes while solving the optimization problem (3.12a) is given by

$$\begin{aligned} \Delta x(k+1) &= \Delta x(k) - T_s v(k) + T_s v_p(k) \\ v(k+1) &= v(k) + T_s a(k). \end{aligned} \tag{3.23}$$

This set of equations is the discretized version of (2.2) with a sampling time, T_s.

3.2.2. Simulation Results

In this section, the defined optimization problem in Section 3.2 with the designed controller from Section 3.2.1 is simulated to showcase the simulation results. To simulate the NMPC controller simple transfer function-based vehicle models are deployed for closed-loop testing purposes. The detailed simulations with the benchmark truck model will be covered extensively in the upcoming chapter.

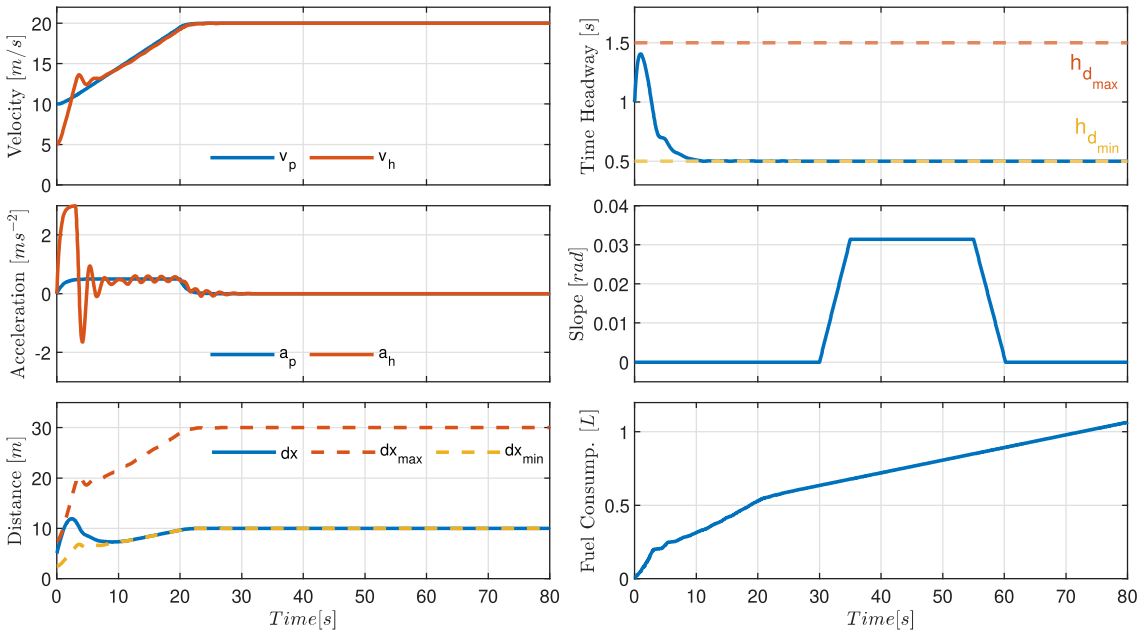

Figure 3.3. Simulation results of CTH strategy.

The following simulations are demonstrated in order to present the idea behind the control design works in principle. In both simulations, the time interval from 30 to 50 seconds contains an uphill section of the road, which is defined by a trapezoidal

shape. Both CTH and ATH strategies are tested with the same road conditions and the same velocity profile of the lead vehicle. The focus of interest of the simulation result will be the time headway behavior and consumed fuel amount by the host vehicle.

In the first simulation, the CTH strategy is tested with a time headway of 0.5 seconds. As results in Figure 3.3 depicts, the host vehicle is able to track the given referenced time headway without considering the uphill road segment and aggressively obeys the constant time headway, which corresponds to 10 meters while the vehicle cruises with 20 mps. In the end, the host truck consumed 1.0658 liters of fuel.

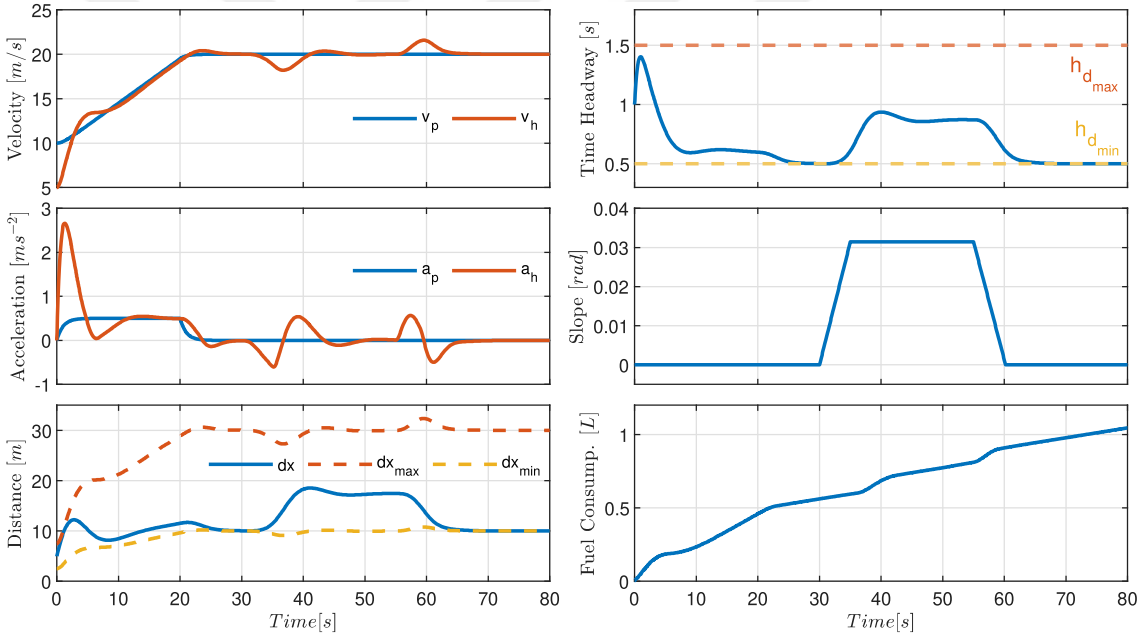

Figure 3.4. Simulation results of ATH strategy.

In the second simulation, the ATH strategy is applied with a time headway envelope of 1 ± 0.5 seconds in which the maximum time headway is 1.5 seconds and the minimum time headway is 0.5 seconds. The results depicted in Figure 3.4 illustrate the dynamic adaptation of the host vehicle's time headway to the lead vehicle throughout the simulation. Notably, during the uphill road section, the time headway gradually increased from 0.5 seconds to approximately 0.9 seconds. This part explains that the optimization problem decided in favor of fuel consumption rather than using the advantage of air drag reduction, which is the core principle underlying our concept.

Once the uphill segment concluded, the time headway was promptly reduced back to 0.5 seconds, allowing the host truck to regain the advantages of the slipstream. At the end of the simulation, the host truck consumed 1.0459 liters of fuel, which is 1.87% less than the first scenario where CTH is applied.

The trial simulations revealed an interesting observation: as the magnitude of the road slope increases, the time headway tends to approach its maximum limit of 1.5 seconds, which aligns with our expectations. This behavior can be attributed to the host vehicle's effort to maintain a constant time headway despite the challenging road conditions. However, it is important to note that this adjustment in time headway also impacts fuel consumption. In instances where the slope is steeper, and the host vehicle endeavors to adhere to the fixed time headway, a higher fuel consumption rate is observed compared to when employing the ATH strategy which underscores the trade-off between maintaining a consistent time headway and optimizing fuel efficiency in varying road conditions.

4. VALIDATION TEST RESULTS UNDER REALISTIC TEST SCENARIOS

Simulation results are obtained in a closed-loop control system environment in MATLAB/Simulink®, where the designed NMPC and the benchmark truck models are integrated and tested together as shown in Figure 4.1. The defined scenarios involve two trucks in a platoon following a predefined velocity profile under different road topography conditions, which are obtained from the map and have real road data (slope and elevation). It is assumed that the lead truck is driven by a driver and the follower truck operates with a Cooperative Adaptive Cruise Control (CACC) system that is under the driver's supervision. As long as the CACC system, which is shown with the green icon in Figure 4.1, is active, the host vehicle is able to adjust its time headway as efficiently as possible.

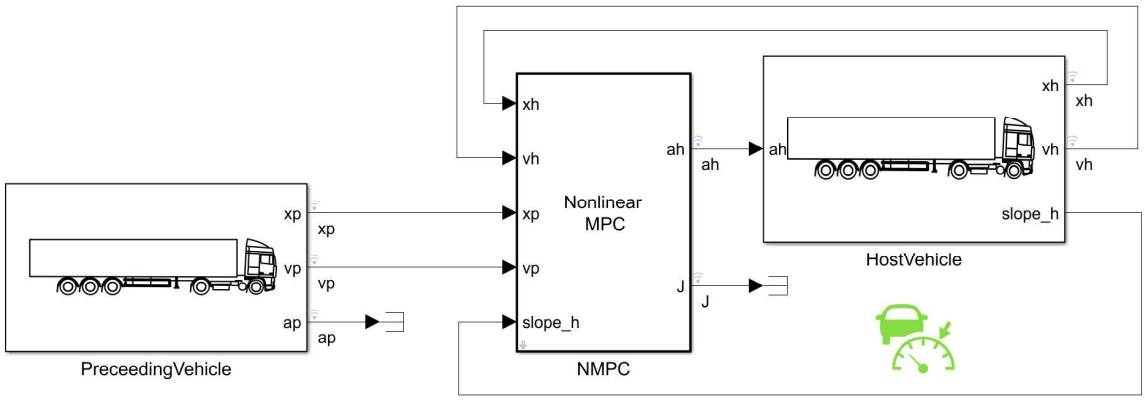

Figure 4.1. Closed-loop simulation system in Simulink.

In the result figures, the first subplot shows the speeds of preceding and host vehicles; the second subplot illustrates the intervehicular distance (Δx) with maximum and minimum boundaries; the third subplot shows the time headway and its defined envelope; the fourth subplot displays the road topography by means of slope and elevation; finally, the fifth subplot illustrates the total fuel consumption of both vehicles.

4.1. Homogeneous Platoon

In this homogeneous platoon scenario, the preceding and host trucks are identical in terms of engine characteristics and have the same load of 40 tons. The simulation begins with both trucks starting in tandem, initialized with the following conditions: the preceding truck's initial position and velocity are set to $x_{p_0} = 15m$ and $v_{p_0} = 0m/s$ respectively, while the host truck's initial position and velocity are $x_{h_0} = 15m$ and $v_{h_0} = 3m/s$. These initial conditions are used consistently throughout all simulations in this section.

There are four simulation scenarios considered, each exploring the effects of constant and adaptive time headway (CTH and ATH) strategies under different road topography conditions. In Scenario 1 and Scenario 2, both CTH and ATH strategies are tested on a flat road without any slopes. This allows for an assessment of the platooning performance under optimal driving conditions. In Scenario 3 and Scenario 4, on the other hand, both CTH and ATH strategies are evaluated on a road that features sections with varying slopes, including uphill and downhill segments. These scenarios provide insights into how the platoon behaves and adapts to changing road conditions and gradients. By analyzing the results from these simulations, valuable information can be obtained regarding the fuel efficiency of the CTH and ATH strategies in different terrains.

4.1.1. Constant Time Headway without Slope (Scenario 1)

Figure 4.2 provides a visual representation of the simulation results obtained under the conditions of a flat road and a constant time headway of 0.5 seconds. The plot demonstrates the performance of the platoon, showcasing how the host vehicle successfully maintains the desired time headway behind the lead truck. This indicates that the platooning system effectively regulates the inter-vehicle distance to achieve the specified constant time headway throughout the simulation. Notably, the fuel consumption of both the lead and host vehicles is captured in this scenario. The lead

vehicle is observed to consume approximately 4.7 liters of fuel, while the host vehicle's fuel consumption amounts to around 4.62 liters. These values highlight the efficient fuel utilization achieved by the platoon, where the host truck has the benefit of reduced drag force which results in lower fuel consumption compared to the lead truck.

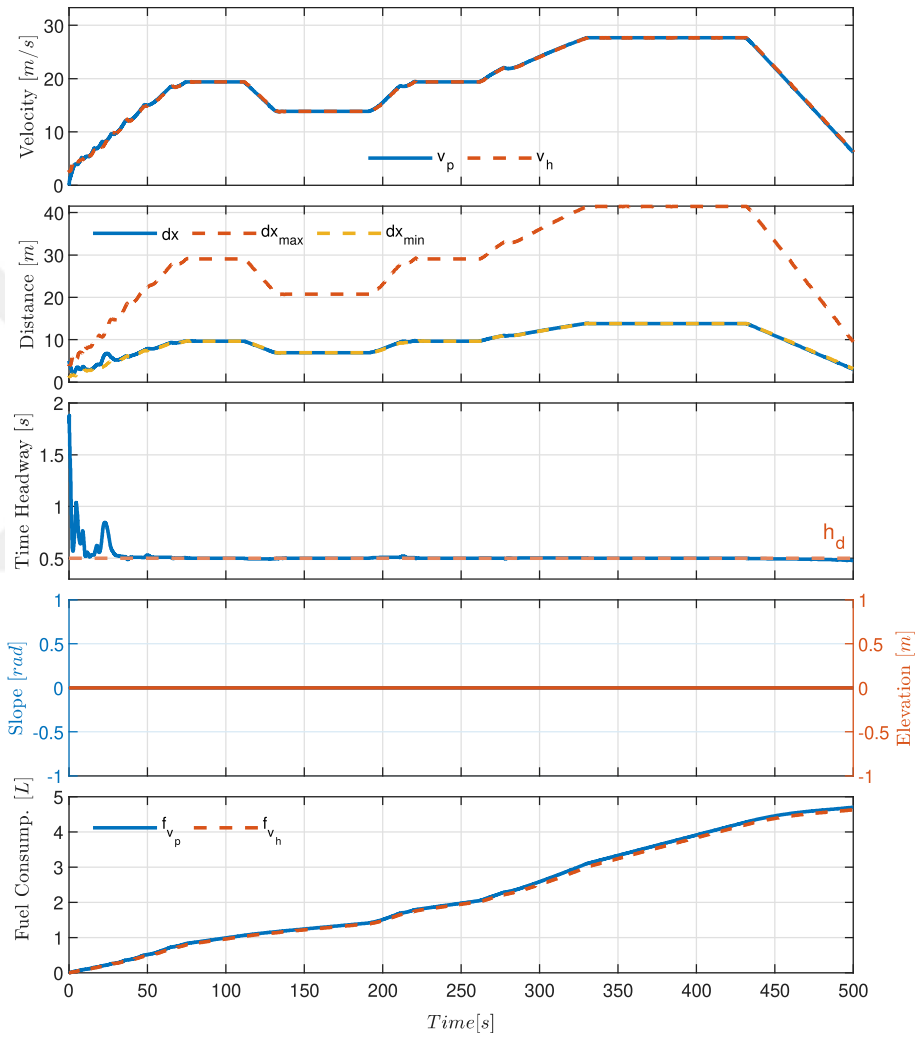

Figure 4.2. Simulation results of homogeneous CTH without slope (Sce. 1).

4.1.2. Adaptive Time Headway without Slope (Scenario 2)

Figure 4.3 presents the simulation results obtained in a scenario where the road remains flat, but the time headway dynamically adjusts within a defined envelope of around 1 second ±0.5 seconds. This adaptive time headway strategy allows the platoon to adapt its inter-vehicle distance according to the prevailing conditions. In

this scenario, the initial time headway is set to 1.5 seconds based on the given initial conditions. Throughout the simulation, the time headway gradually decreases to its minimum limit within the time range of 0-120 seconds. Notably, the host vehicle exhibits a tendency to increase the time headway during acceleration periods, which occur between 200-350 seconds. Conversely, during deceleration and constant cruising phases, observed between 120-200 seconds and 350-500 seconds respectively, the host vehicle aims to maintain the smallest time headway possible. Analyzing the simulation results, it is observed that the lead vehicle consumes approximately 4.7 liters of fuel, while the host vehicle achieves a fuel consumption of around 4.56 liters. These findings indicate that with the adaptively changing time headway strategy, the host vehicle can reduce its fuel consumption even more than the CTH strategy.

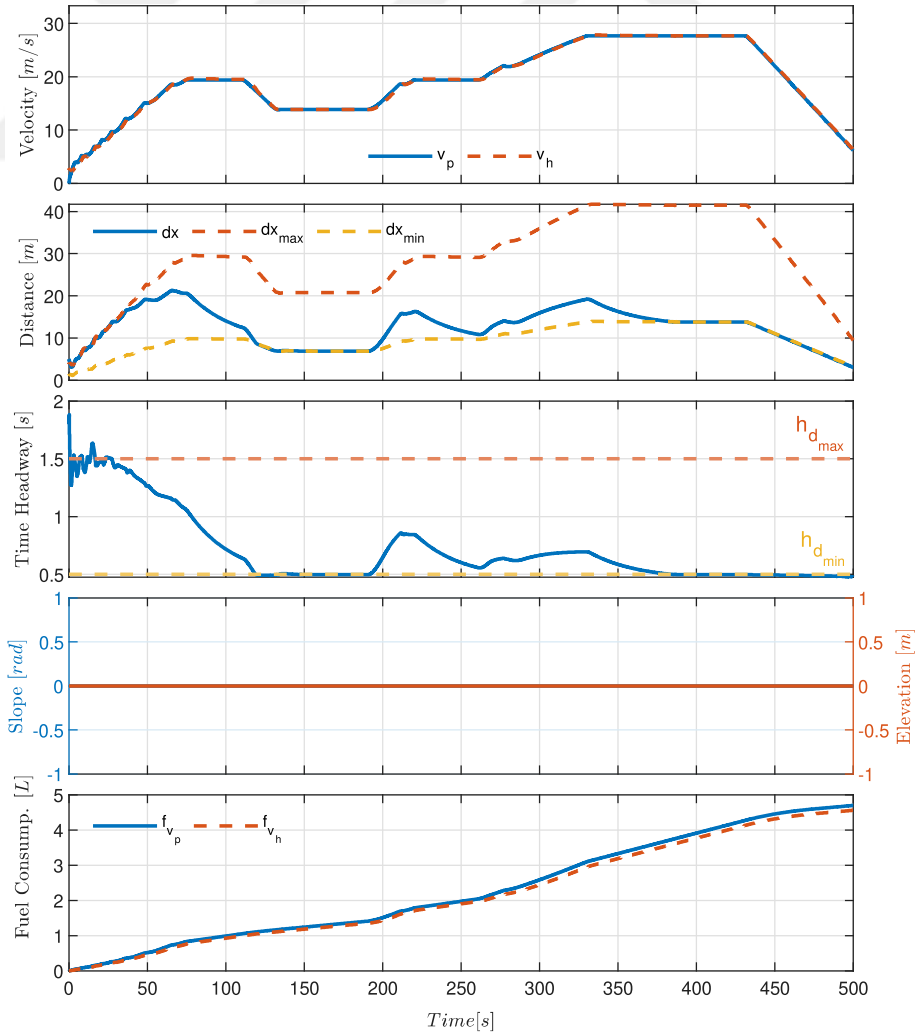

Figure 4.3. Simulation results of homogeneous ATH without slope (Sce. 2).

4.1.3. Constant Time Headway with Slope (Scenario 3)

Figure 4.4 presents the simulation results of a scenario where the road consists of both uphill and downhill sections, while the commanded time headway is kept constant at 0.5 seconds, which the host vehicle diligently attempts to track. The purpose of this scenario is to provide a comparative analysis against the ATH case.The subplots in Figure 4.4 clearly illustrate that regardless of the slope conditions, the designed controller successfully maintains a constant time headway between the lead and host vehicles. This demonstrates the robustness and effectiveness of the controller in adapting to varying road gradients while ensuring the desired spacing is maintained.

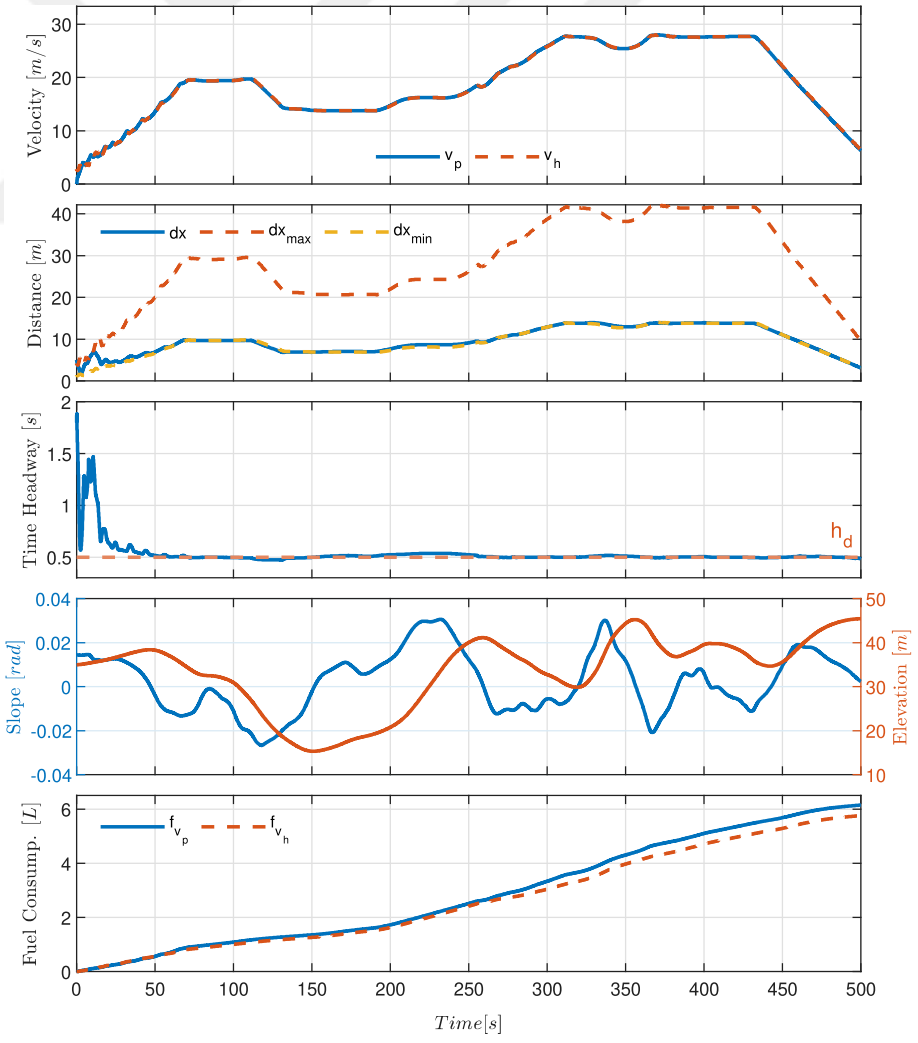

Figure 4.4. Simulation results of homogeneous CTH with slope (Sce. 3).

Analyzing the simulation results, it is evident that the lead vehicle consumes approximately 6.15 liters of fuel, while the host vehicle achieves fuel consumption of around 5.76 liters. These findings indicate that even under challenging uphill and downhill road conditions, the platooning system managed to maintain the commanded time headway, resulting in noteworthy fuel efficiency.

4.1.4. Adaptive Time Headway with Slope (Scenario 4)

Figure 4.5 provides a comprehensive overview of the simulation results for a scenario where the road consists of both uphill and downhill sections, while the time headway is adaptively changing within a defined envelope. This particular case incorporates various factors such as slope, acceleration, and deceleration, which influence the host vehicle's distance adjustment with respect to the preceding truck.

Analyzing the subplots in Figure 4.5, we can observe the dynamic behavior of the host vehicle in response to the changing road conditions. Between 0 and 100 seconds, the host truck effectively leverages the downhill section, allowing it to decrease the time headway and reach the minimum limit of 0.5 seconds. This shorter time headway is maintained until approximately 150 seconds, taking advantage of the favorable terrain. At around 150 seconds, an uphill section is encountered, which prompts the host vehicle to initiate an acceleration pattern until 250 seconds. During this phase, the time headway gradually increases, reaching up to 1 second. This adjustment allows the host vehicle to maintain a safe distance while navigating the uphill section. Between 260 and 325 seconds, a downhill section emerges, enabling the host truck to close the gap and reduce the time headway once again before the upcoming uphill section. Subsequently, another downhill section followed by a deceleration pattern is observed starting around 350 seconds. Throughout this period, the time headway is consistently kept at the lowest limit of 0.5 seconds until the end of the simulation. It is observed from the results that the lead vehicle consumes approximately 6.15 liters of fuel, while the host vehicle consumes around 4.66 liters.

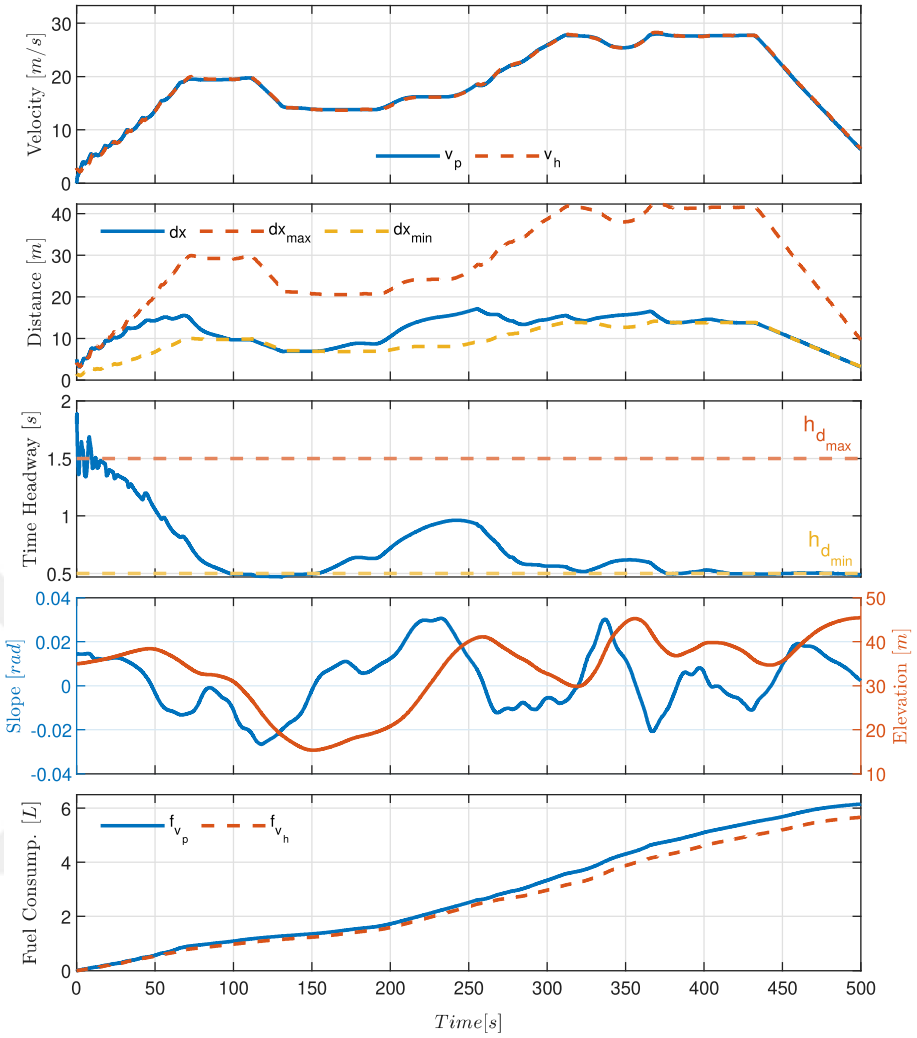

Figure 4.5. Simulation results of homogeneous ATH with slope (Sce. 4).

4.2. Heterogeneous Platoon

In the heterogeneous platoon scenario, the preceding and host have the same engine characteristics but differ in terms of their loads of 35 and 40 tons, respectively. The simulation starts with both trucks commencing their journey in synchrony, and they are assigned distinct initial conditions. The preceding truck begins with an initial position of $x_{p_0} = 15m$ and a velocity of $v_{p_0} = 0m/s$, while the host truck starts with an initial position of $x_{h_0} = 15m$ and a velocity of $v_{h_0} = 3m/s$. These specific initial conditions are consistently applied across all simulations conducted in this section.

The simulations encompass four distinct scenarios, each exploring the effects of constant and adaptive time headway (CTH and ATH) strategies in diverse road topography conditions. In Scenario 5 and Scenario 6, both CTH and ATH strategies are tested on a flat road, devoid of any slopes. In contrast, Scenario 7 and Scenario 8 focus on evaluating both CTH and ATH strategies on a road featuring varying slopes, including uphill and downhill sections.

By analyzing the results obtained from these simulations, we can gain a deeper understanding of the fuel efficiency implications associated with the utilization of CTH and ATH strategies in different truck tandems and road conditions. That is why the focus of interest in this section is to compare the fuel consumption of host vehicles under different spacing strategies. We would like to observe the difference in the host truck's behavior and fuel consumption metrics specific to CTH and ATH strategies.

4.2.1. Constant Time Headway without Slope (Scenario 5)

Figure 4.6 presents a comprehensive visualization of the simulation results achieved on a flat road, with a constant time headway of 0.5 seconds implemented within the heterogeneous platoon. The plot effectively illustrates the performance of the platoon, demonstrating the host vehicle's successful ability to maintain the desired time headway behind the lead truck throughout the simulation duration.

Of particular interest are the fuel consumption findings for the host vehicle, which amount to approximately 4.71 liters, or equivalently, an estimated 48.73 liters per 100 kilometers. These results serve as a valuable baseline for comparison, setting the stage for the subsequent scenario where the adaptive time headway (ATH) strategy is employed under the same road conditions. By contrasting the outcomes of the ATH strategy against those of the constant time headway (CTH) strategy, a deeper understanding can be gained regarding the potential fuel efficiency improvements and overall platooning performance achievable with adaptive strategies in a heterogeneous platoon setting.

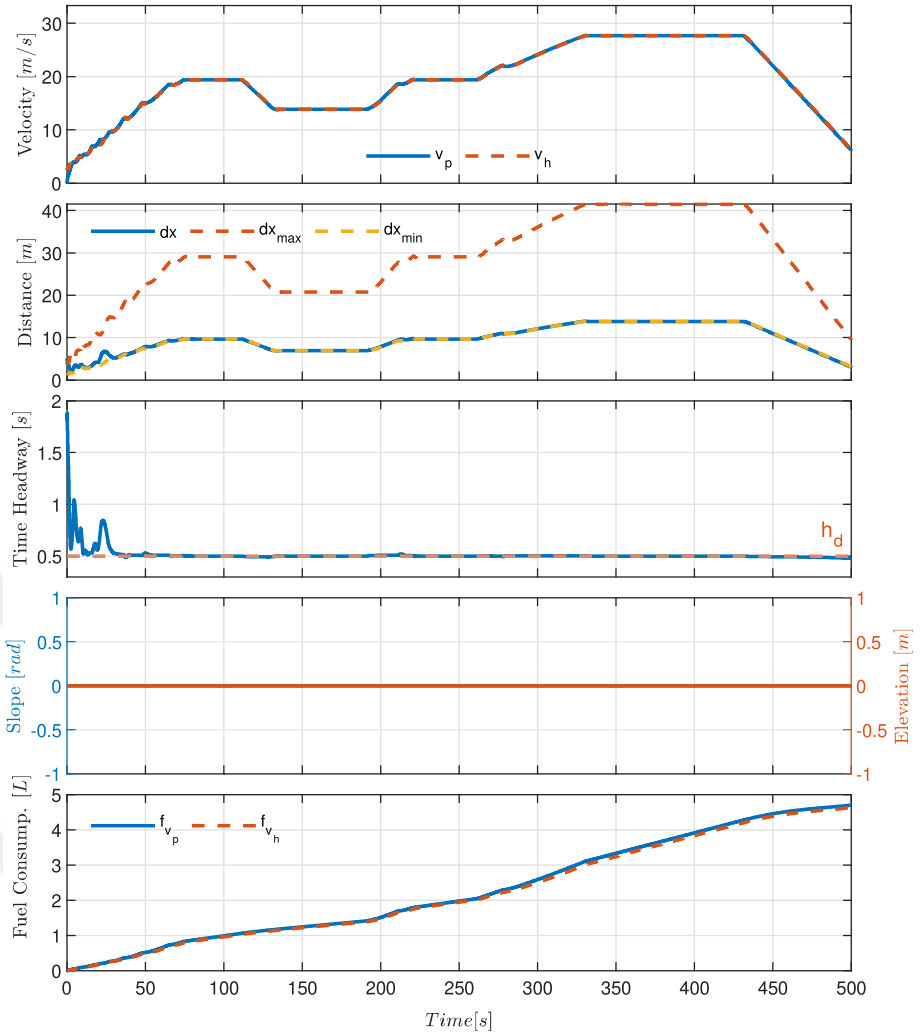

Figure 4.6. Simulation results of heterogeneous CTH without slope (Sce. 5).

4.2.2. Adaptive Time Headway without Slope (Scenario 6)

In an attempt to determine whether the adaptive time headway (ATH) strategy surpasses the constant time headway (CTH) approach in terms of efficiency, the ATH strategy is implemented on the host vehicle within the heterogeneous platoon. Fig. 4.7 provides a visual representation of the simulation results, highlighting the dynamic adjustments made to the time headway throughout the simulation.

As observed in the plot, the ATH strategy allows for the optimization of the intervehicular distance by enabling the heavy host vehicle to increase the gap during acceleration phases while closing it during deceleration and periods of constant speed.

These findings underscore the advantage of employing a flexible approach rather than adhering strictly to a fixed time headway. The results indicate that the optimization problem favors adaptability in response to varying road conditions and driving situations. Notably, the fuel consumption analysis reveals that, under the ATH strategy, the host truck consumed approximately 4.61 liters of fuel, which translates to an estimated 47.63 liters per 100 kilometers. These results highlight the potential fuel efficiency gains achievable through the utilization of adaptive strategies within a heterogeneous platoon.

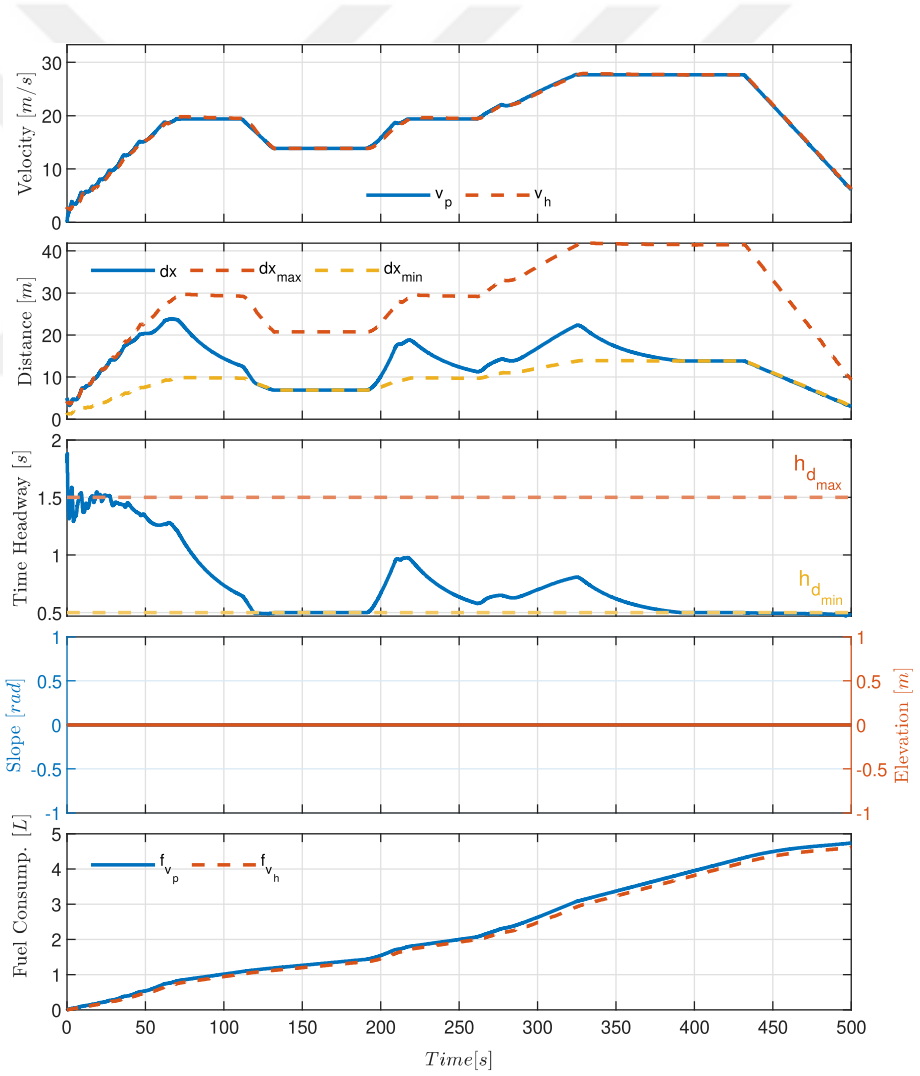

Figure 4.7. Simulation results of heterogeneous ATH without slope (Sce. 6).

4.2.3. Constant Time Headway with Slope (Scenario 7)

The constant time headway (CTH) strategy is implemented in the host vehicle of the heterogeneous platoon to explore the implications of maintaining a strict time headway target while cruising on a road. The objective is to observe the behavior and performance of the host vehicle in relation to the preceding truck. Figure 4.8 visually presents the outcomes of this scenario, illustrating how the host vehicle maintains a consistent distance of 0.5 seconds from the preceding truck throughout the simulation. It is worth noting that the preceding truck in this scenario carries a lighter load, enabling it to achieve faster acceleration capabilities compared to the host vehicle.

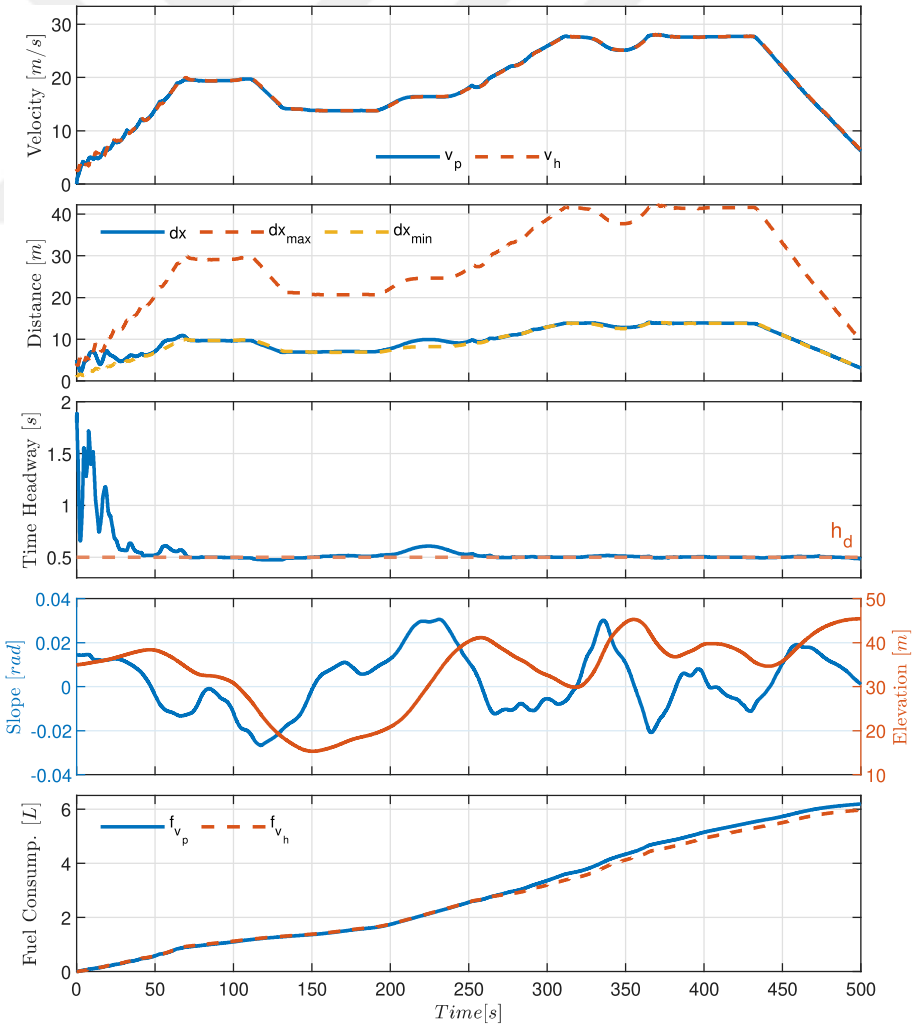

Figure 4.8. Simulation results of heterogeneous CTH with slope (Sce. 7).

This imbalance in performance between the vehicles raises the question of whether the constant time headway strategy is truly beneficial for the host vehicle in a heterogeneous platoon setting. Analyzing the results obtained from this scenario, we observe that the host truck consumes 5.97 liters of fuel. When extrapolated, this corresponds to an estimated fuel consumption rate of 62.96 liters per 100 kilometers. These findings serve as a critical reference point for further comparison.

4.2.4. Adaptive Time Headway with Slope (Scenario 8)

In an effort to evaluate whether the adaptive time headway (ATH) strategy surpasses the constant time headway (CTH) approach in terms of efficiency within the context of a heterogeneous platoon, the ATH strategy is implemented on the host vehicle.

Figure 4.9 visually presents the simulation results, showcasing the dynamic adjustments made to the time headway throughout the simulation. As illustrated in the plot, the ATH strategy enables the heavy host vehicle to adapt its time headway to optimize intervehicular distance management. Notably, during uphill sections, the host vehicle allows for a larger gap between itself and the preceding truck, recognizing that maintaining close proximity may not be the most fuel-efficient approach. Conversely, during downhill or deceleration sections of the road, the host vehicle closes the gap, maximizing the benefits of reduced resistance and improved fuel economy. A comparison between Scenario 4 and the current scenario clearly reveals that the time headway increases between 150-300 seconds, reflecting the host vehicle's decision to prioritize fuel consumption efficiency while climbing uphill. Remarkably, under the ATH strategy, the host truck consumed approximately 5.79 liters of fuel, projecting to be around 61.1 liters per 100 kilometers.

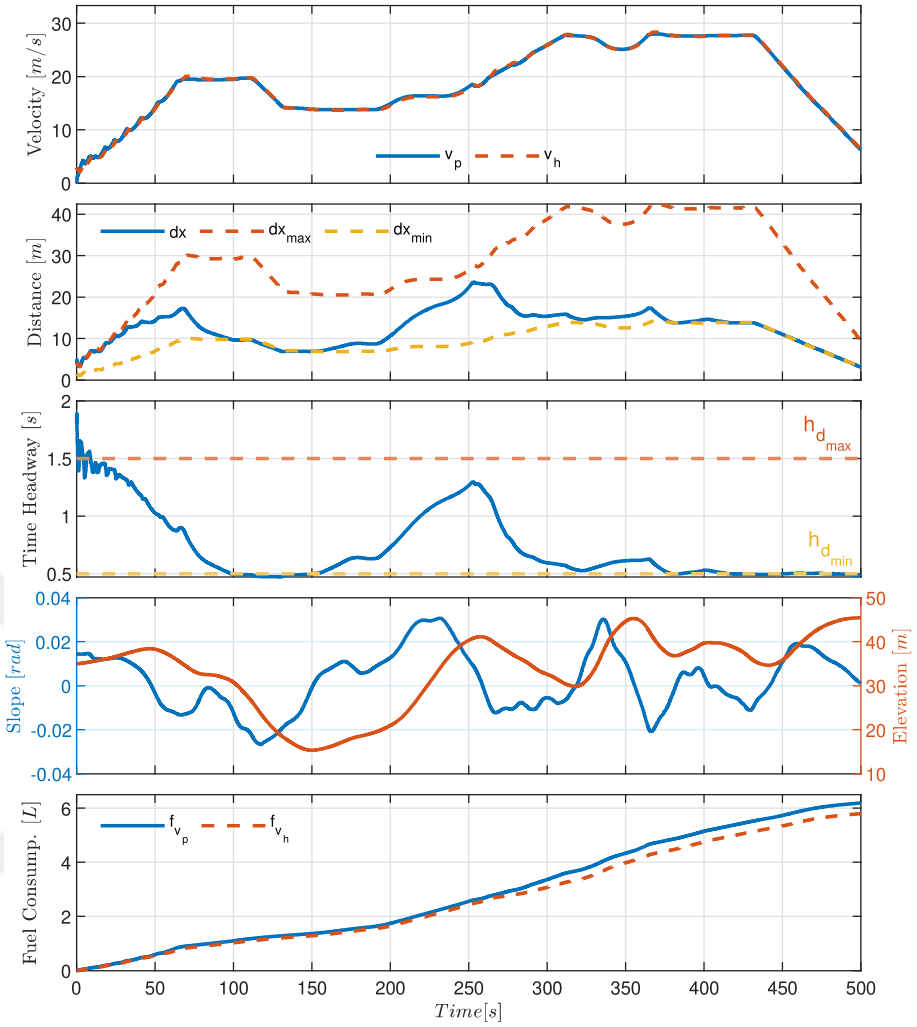

Figure 4.9. Simulation results of heterogeneous ATH with slope (Sce. 8).

4.3. Evaluation of the Simulation Results

In this section, we comprehensively discuss the fuel consumption results obtained from the eight simulation scenarios, along with specific highlights pertaining to each scenario. Figure 4.10 presents the time headway behaviors of homogeneous and heterogeneous platoons under the specified strategy (CTH or ATH) and different road conditions. In the legend of the subplots, superscript ($\sim$) explains the time headway of heterogeneous platoon, and subscript (s) indicates the road with up and down slopes. If time headway (τ) is alone, it states a homogeneous platoon formation on a flat road. The subplots on the left-hand side in 4.10 show the time headway results of the CTH strategy while the ones on the right show the results of the ATH strategy.

Based on the simulation results, the application of the adaptive time headway (ATH) strategy reveals distinct time headway behaviors between homogeneous and heterogeneous platoons. In the case of a flat road scenario, it is observed that the time headway for heterogeneous formation is slightly larger than that of the homogeneous formation. This variation indicates that maintaining a closer distance to a lighter lead vehicle is not always the most fuel-efficient option due to increased control effort, leading to higher fuel consumption. Consequently, the margin of the time headway is greater for heterogeneous formations. Similar observations hold true for scenarios involving roads with up and down slopes, where the time headway is further increased for heterogeneous formations compared to homogeneous formations. On the other hand, there is not much to observe in the CTH since a constant time headway is achieved by the controller all the time without considering any changes in platoon type and road conditions.

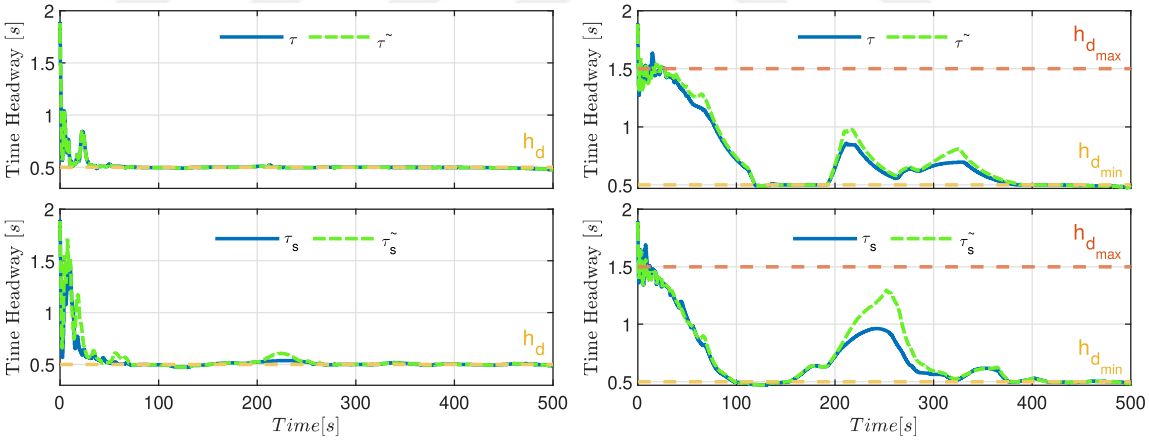

Figure 4.10. Combined time headway results of different scenarios.

As a result, the increased time headway for heterogeneous platoons results in a higher fuel reduction for the host vehicles while the constant time headway for heterogeneous platoons caused more fuel consumption. The fuel consumption metrics can be seen in Figure 4.11 and the comparison of the CTH and ATH strategies is visible in Table 4.1.

Figure 4.11 provides an insightful visualization of the actual and projected fuel consumption, presented as the fuel consumption per 100 kilometers, for all scenarios. To facilitate analysis, the figure is divided by a dashed separation line, with the left-hand side representing the homogeneous platoon scenarios (Scenario 1 - Scenario 4), and the right-hand side depicting the heterogeneous platoon scenarios (Scenario 5 - Scenario 8). By examining the fuel consumption summary and drawing attention to noteworthy observations within each scenario, we aim to gain a deeper understanding of the impact of our proposed approach on fuel efficiency in different platooning formations. Additionally, we quantify the fuel benefits achieved by comparing the fuel consumption of the host vehicle with that of the preceding vehicle and by comparing the adaptive time headway (ATH) strategy with the constant time headway (CTH) strategy. The summary of these fuel benefits, presented as percentage values, is provided in Table 4.1, further elucidating the advantages of our approach in reducing fuel consumption in heavy-duty vehicle platooning scenarios.

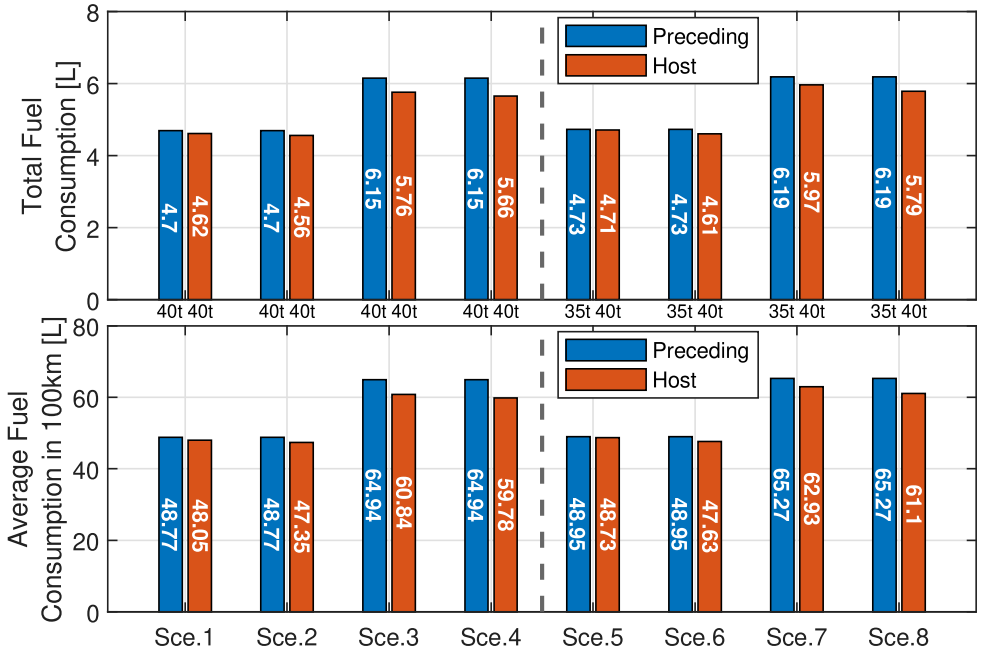

Figure 4.11. Scenario specific fuel consumption results.

In Scenario 1, where the road is flat, the host vehicle capitalized on the advantageous reduction in air drag force facilitated by the homogeneous platoon formation under the constant time headway (CTH) strategy. As a result, the host vehicle con-

sumed 4.66 L of fuel, while the preceding vehicle consumed 4.7 L, representing a 1.7% fuel benefit for the host vehicle compared to the preceding vehicle. This differentiation is further emphasized when considering the projected fuel consumption metrics per 100 km, with the preceding vehicle consuming 48.77 liters of fuel and the host vehicle consuming 48.05 liters. This equates to an approximate 1.48% fuel benefit for the host vehicle.

In Scenario 2, characterized by a flat road, we implemented the adaptive time headway (ATH) strategy for the host vehicle within a homogeneous platoon. In this configuration, the fuel consumption of the host vehicle was measured at 4.56 liters. Projecting this value to a consumption rate per 100 km, we obtained a figure of 47.35 liters. In contrast, the preceding vehicle recorded a fuel consumption of 4.7 liters, corresponding to a projected consumption of 48.77 liters per 100 km. These findings demonstrate a notable actual fuel benefit of 2.9% for the host vehicle, with a similar projected benefit of 2.91% over a distance of 100 km. These findings reinforce the effectiveness of the platoon formation and the ATH strategy in achieving fuel efficiency improvements for the host vehicle compared to its preceding counterpart. For the first two scenarios, it can be observed that the ATH strategy is better than the CTH strategy by 1.36% actual and 1.46% projected in fuel efficiency.

In Scenario 3, where the road has slopes and the platoon is homogeneous, the host vehicle consumed 5.76 L of fuel, while the preceding vehicle consumed 6.15 L, representing a 6.34% fuel benefit for the host vehicle compared to the preceding vehicle. This differentiation is further emphasized when considering the projected fuel consumption metrics per 100 km, with the preceding vehicle consuming 64.94 liters of fuel and the host vehicle consuming 60.84 liters. This equates to an approximate 6.31% fuel benefit for the host vehicle.

In Scenario 4, characterized by a road with up and down slopes, we implemented the adaptive time headway (ATH) strategy for the host vehicle within a homogeneous platoon. In this configuration, the fuel consumption of the host vehicle was measured

at 5.66 liters. Projecting this value to a consumption rate per 100 km, we obtained a figure of 59.78 liters. In contrast, the preceding vehicle recorded a fuel consumption of 6.15 liters, corresponding to a projected consumption of 64.94 liters per 100 km. These findings demonstrate an actual fuel benefit of 7.97% for the host vehicle, with a similar projected benefit of 7.95% over a distance of 100 km.

Table 4.1. Fuel benefit of a host vehicle compared to preceding vehicle under different spacing strategies.

Comparison	**Actual Fuel Benefit**	**Fuel Benefit in 100km**
Preceding vs Host Vehicle		
Scenario 1	1.70%	1.48%
Scenario 2	2.98%	2.91%
Scenario 3	6.34%	6.31%
Scenario 4	7.97%	7.95%
Scenario 5	0.42%	0.45%
Scenario 6	2.54%	2.70%
Scenario 7	3.55%	3.59%
Scenario 8	6.46%	6.39%
Constant vs Adaptive Time Headway		
Sce. 1 vs Sce. 2	1.30%	1.46%
Sce. 3 vs Sce. 4	1.74%	1.74%
Sce. 5 vs Sce. 6	2.12%	2.26%
Sce. 7 vs Sce. 8	3.02%	2.91%

In Scenario 5, where the road is flat, the host vehicle capitalized on the advantageous reduction in air drag force facilitated by the heterogeneous platoon formation under the constant time headway (CTH) strategy. As a result, the host vehicle consumed 4.71 L of fuel, while the preceding vehicle consumed 4.73 L, representing a 0.42% fuel benefit for the host vehicle compared to the preceding vehicle. This differentiation

is further emphasized when considering the projected fuel consumption metrics per 100 km, with the preceding vehicle consuming 48.95 liters of fuel and the host vehicle consuming 48.73 liters. This equates to an approximate 0.45% fuel benefit for the host vehicle.

In Scenario 6, characterized by a flat road, we implemented the adaptive time headway (ATH) strategy for the host vehicle within a heterogeneous platoon. In this configuration, the fuel consumption of the host vehicle was measured at 4.61 liters. Projecting this value to a consumption rate per 100 km, we obtained a figure of 47.63 liters. In contrast, the preceding vehicle recorded a fuel consumption of 4.73 liters, corresponding to a projected consumption of 48.95 liters per 100 km. These findings demonstrate a notable actual fuel benefit of 2.54% for the host vehicle, with a similar projected benefit of 2.70% over a distance of 100 km.

These findings reinforce the effectiveness of the platoon formation and the ATH strategy in achieving fuel efficiency improvements for the host vehicle. For Scenarios 5 and 6, it can be observed that the ATH strategy is better than the CTH strategy by 2.12% actual and 2.26% projected in fuel efficiency.

In Scenario 7, characterized by a road with slopes and a heterogeneous platoon, the host vehicle demonstrated significant fuel efficiency by consuming 5.97 liters, while the preceding vehicle consumed 6.19 liters. This marked difference translates to a substantial 3.55% fuel benefit for the host vehicle over its preceding counterpart. The significance of this advantage becomes even more pronounced when examining the projected fuel consumption per 100 km, where the preceding vehicle consumes 65.27 liters, while the host vehicle consumes 62.93 liters, resulting in an approximate 3.59% fuel benefit for the host vehicle.

In Scenario 8, which features a road with varying slopes, we implemented the adaptive time headway (ATH) strategy for the host vehicle within a heterogeneous platoon. In this setting, the host vehicle consumed 5.78 liters of fuel, equivalent to

a projected consumption of 61.1 liters per 100 km. In contrast, the preceding vehicle consumed 6.19 liters, corresponding to a projected consumption of 65.27 liters per 100 km. These results clearly demonstrate an actual fuel benefit of 6.46% for the host vehicle, with a similar projected benefit of 6.39% over a distance of 100 km.

Examining Scenarios 7 and 8 collectively underscores the advantages of platoon formation and the utilization of reduced air drag, as the host vehicle consistently achieved lower fuel consumption compared to its preceding counterpart. Moreover, the adoption of the ATH strategy delivered notable fuel efficiency improvements of 2.12% on a flat road and 3.02% on a road with slopes when compared to the constant time headway (CTH) strategy. These findings highlight the substantial benefits that can be attained by employing the ATH strategy in real-world platooning scenarios.

The fuel consumption results demonstrate that the adaptive time headway (ATH) strategy consistently outperforms the constant time headway (CTH) strategy in both homogeneous and heterogeneous platoon scenarios. Regardless of the platooning configuration, the host vehicle consistently consumes less fuel than its preceding counterpart. This highlights the inherent advantage of platoon formation in reducing air drag and improving fuel efficiency. Specifically, when comparing the fuel consumption of the host vehicle under ATH and CTH strategies, it is evident that the ATH strategy consistently leads to lower fuel consumption. The observed trend reinforces the effectiveness of the ATH strategy in optimizing intervehicular distances and adapting to varying traffic conditions.

5. CONCLUSION AND FUTURE WORK

Vehicle platoon control is a complex control problem, especially when dealing with a platoon consisting of two or more vehicles with nonlinear characteristics. Ensuring efficient operation and coordination within the platoon remains a challenging task. Additionally, real-life applications of vehicle platooning encounter unresolved issues related to spacing strategies and the fuel consumption or efficiency of the vehicles in the platoon.

This thesis has presented a comprehensive investigation into the field of HDV platooning and spacing policy-based fuel-efficient control strategies. The main contribution of this thesis has been to develop an innovative adaptive time headway strategy that adjusts the intervehicular distance dynamically based on the trade-off between the possible gain from the air drag reduction and focusing only on lowering fuel consumption. In order to achieve fuel consumption reduction, the decision out of the optimization problem that is solved by NMPC is applied to the system. The incorporation of the nonlinear fuel consumption model and the nonlinear air drag model into the optimization process ensures the effective minimization of fuel consumption while maintaining a safe and stable distance between the trucks without breaking their formation. A robust control strategy was successfully developed, implemented, and tested.

Another contribution of this work is to integrate nonlinear dynamics and nonquadratic cost function terms into the control design rather than relying on the linearized dynamics and quadratic cost function terms for linear controller design. The main reason behind this is the fact that the expected gains from the proposed control method were not high due to the nature of the problem. Therefore, simplifying the models for linear MPC implementation could have resulted in a loss of achievable benefits.

In addition to the aforementioned contributions, this work also includes an assessment of both the adaptive time headway (ATH) and constant time headway (CTH) strategies. The performance of the proposed adaptive time headway approach for heavy-duty vehicle platoons is compared to that of the constant time headway approach. Through extensive simulations, the results clearly demonstrate that the designed NMPC controller with the adaptive time headway strategy effectively reduces fuel consumption to a greater extent compared to the constant time headway strategy. Moreover, the behavior of the designed ATH strategy is tested under different road topography conditions to exhibit its capability of reducing fuel consumption.

Comprehensive simulations are also conducted with benchmark truck models to validate the effectiveness and robustness of the suggested approach. The control design was initially tested with linear, transfer function-based vehicle models; however, those have been used to verify the initial design and replaced with benchmark truck models later on for realistic validation test scenarios. It is observed that the designed approach also works with complex plant models and achieves the expected reduction in fuel consumption.

In conclusion, this thesis successfully developed and implemented a nonlinear model predictive control-based adaptive time headway strategy for fuel-efficient HDV platooning. The adaptive time headway strategy demonstrated its effectiveness in improving fuel efficiency in both homogeneous and heterogeneous platoon scenarios. Compared to the constant time headway strategy, the host truck achieved a fuel efficiency improvement of 3%. Furthermore, when compared to the lead vehicle, the host truck achieved a remarkable fuel efficiency improvement of 8%. These findings highlight the potential of the adaptive time headway strategy in significantly reducing fuel consumption in heavy-duty truck platooning scenarios. Finally, the contributions made in this thesis offer valuable insights and lay the foundation for future advancements in the field of HDV platooning and fuel-efficient control strategies.

The simulation results validate the effectiveness of the proposed adaptive time headway strategy and highlight its potential for fuel efficiency improvements in HDV platooning. However, there are several areas for future research. Firstly, the application of the same adaptive time headway strategy on a longer platoon formation can be further investigated by also considering the string stability effect. Secondly, investigating the impact of different road and traffic conditions on the adaptive time headway strategy will provide valuable insights for further optimization. Additionally, exploring the synergies between the adaptive time headway strategy and emerging technologies like electric and autonomous vehicles can unlock new possibilities for enhanced fuel efficiency and sustainability in HDV platooning. Finally, a promising avenue to explore is the integration of a hybrid model predictive control approach, which combines both discrete and continuous control actions and considers gear shifting in HDV platooning. Gear shifting plays a crucial role in the overall fuel efficiency of heavy-duty vehicles, and incorporating it into the control strategy can lead to further improvements.

REFERENCES

1. International Transport Forum, *Freight Transport: Bold Action Can Decarbonise Movement of Goods*, OECD Publishing, Paris, 2021.

2. Sivanandham, S. and M. S. Gajanand, "Platooning for Sustainable Freight Transportation: An Adoptable Practice in the Near Future?", *Transport Reviews*, Vol. 40, No. 5, pp. 581–606, 2020.

3. Demir, E., T. Bektaş and G. Laporte, "A Review of Recent Research on Green Road Freight Transportation", *European Journal of Operational Research*, Vol. 237, No. 3, pp. 775–793, 2014.

4. Alam, A., B. Besselink, V. Turri, J. MåRtensson and K. H. Johansson, "Heavy-Duty Vehicle Platooning for Sustainable Freight Transportation: A Cooperative Method to Enhance Safety and Efficiency", *IEEE Control Systems Magazine*, Vol. 35, No. 6, pp. 34–56, 2015.

5. Browand, F., J. McArthur and C. Radovich, *Fuel Saving Achieved in the Field Test of Two Tandem Trucks*, California Partners for Advanced Transit and Highways (PATH), Los Angeles, 2004.

6. Ploeg, J., S. Shladover, H. Nijmeijer and N. van de Wouw, "Introduction to the Special Issue on the 2011 Grand Cooperative Driving Challenge", *IEEE Transactions on Intelligent Transportation Systems*, Vol. 13, No. 3, pp. 989–993, 2012.

7. Alam, A., J. Mårtensson and K. H. Johansson, "Experimental Evaluation of Decentralized Cooperative Cruise Control for Heavy-Duty Vehicle Platooning", *Control Engineering Practice*, Vol. 38, pp. 11–25, 2015.

8. PATH, "California Partners for Advanced Transportation Technology", 1986, `https://path.berkeley.edu/home`, accessed on December 12, 2022.

9. McMahon, D. H., J. K. Hedrick and S. E. Shladover, "Vehicle Modelling and Control for Automated Highway Systems", *American Control Conference*, San Diego, CA, USA, pp. 297–303, 1990.

10. Singh, S., *Critical Reasons for Crashes Investigated in the National Motor Vehicle Crash Causation Survey*, NHTSA's National Center for Statistics and Analysis, Washington, 2018.

11. Robinson, T., E. Chan and E. Coelingh, "An Introduction to the SARTRE Platooning Programme", *17th World Congress on Intelligent Transport Systems*, Busan, South Korea, pp. 1–11, 2010.

12. Wang, Z., G. Wu and M. J. Barth, "A Review on Cooperative Adaptive Cruise Control (CACC) Systems: Architectures, Controls, and Applications", *21st International Conference on Intelligent Transportation Systems (ITSC)*, Hawaii, HI, USA, pp. 2884–2891, 2018.

13. Nieuwenhuijze, M. R. I., T. van Keulen, S. Öncü, B. Bonsen and H. Nijmeijer, "Cooperative Driving With a Heavy-Duty Truck in Mixed Traffic: Experimental Results", *IEEE Transactions on Intelligent Transportation Systems*, Vol. 13, No. 3, pp. 1026–1032, 2012.

14. Englund, C., L. Chen, J. Ploeg, E. Semsar-Kazerooni, A. Voronov, H. H. Bengtsson and J. Didoff, "The Grand Cooperative Driving Challenge 2016: Boosting the Introduction of Cooperative Automated Vehicles", *IEEE Wireless Communications*, Vol. 23, No. 4, pp. 146–152, 2016.

15. Naus, G. J. L., R. P. A. Vugts, J. Ploeg, M. J. G. van de Molengraft and M. Steinbuch, "String-Stable CACC Design and Experimental Validation: A Frequency-Domain Approach", *IEEE Transactions on Vehicular Technology*, Vol. 59, No. 9, pp. 4268–4279, 2010.

16. Schindler, R., M. Jänsch, A. Bálint and H. Johannsen, "Exploring European Heavy Goods Vehicle Crashes Using a Three-Level Analysis of Crash Data", *International Journal of Environmental Research and Public Health*, Vol. 19, No. 2, pp. 663–680, 2022.

17. Alam, A., J. Mårtensson and K. H. Johansson, "Look-Ahead Cruise Control For Heavy Duty Vehicle Platooning", *16th International IEEE Conference on Intelligent Transportation Systems*, The Hague, Netherlands, pp. 928–935, 2013.

18. Turri, V., B. Besselink, J. Mårtensson and K. H. Johansson, "Fuel-Efficient Heavy-Duty Vehicle Platooning by Look-Ahead Control", *53rd IEEE Conference on Decision and Control*, Los Angeles, LA, USA, pp. 654–660, 2014.

19. Turri, V., B. Besselink and K. H. Johansson, "Cooperative Look-Ahead Control for Fuel-Efficient and Safe Heavy-Duty Vehicle Platooning", *IEEE Transactions on Control Systems Technology*, Vol. 25, No. 1, pp. 12–28, 2017.

20. Jiang, D. and L. Delgrossi, "IEEE 802.11p: Towards an International Standard for Wireless Access in Vehicular Environments", *IEEE Vehicular Technology Conference*, Marianna Bay, Singapore, pp. 2036–2040, 2008.

21. European Commission, "Harmonisation of the 5.9 GHz Spectrum Band for Real-Time Information Exchange Will Improve Road And Urban Rail Transport Safety", 2020, `https://digital-strategy.ec.europa.eu/en/news`, accessed on February 21, 2023.

22. Wu, C., Z. Xu, Y. Liu, C. Fu, K. Li and M. Hu, "Spacing Policies for Adaptive Cruise Control: A Survey", *IEEE Access*, Vol. 8, pp. 50149–50162, 2020.

23. Öncü, S., J. Ploeg, N. van de Wouw and H. Nijmeijer, "Cooperative Adaptive Cruise Control: Network-Aware Analysis of String Stability", *IEEE Transactions on Intelligent Transportation Systems*, Vol. 15, No. 4, pp. 1527–1537, 2014.

24. Wang, J. and R. Rajamani, "Adaptive Cruise Control System Design and Its Impact on Highway Traffic Flow", *Proceedings of American Control Conference*, Anchorage, AK, USA, pp. 3690–3695, 2002.

25. Sancar, F. E., B. Fidan, J. P. Huissoon and S. L. Waslander, "MPC Based Collaborative Adaptive Cruise Control with Rear End Collision Avoidance", *IEEE Intelligent Vehicles Symposium Proceedings*, Dearborn, MI, USA, pp. 516–521, 2014.

26. Swaroop, D. and J. K. Hedrick, "Constant Spacing Strategies for Platooning in Automated Highway Systems", *Journal of Dynamic Systems, Measurement, and Control*, Vol. 121, No. 3, pp. 462–470, 1999.

27. Swaroop, D., J. K. Hedrick, C. Chien and P. Ioannou, "A Comparison of Spacing and Headway Control Laws for Automatically Controlled Vehicles", *Vehicle System Dynamics*, Vol. 23, No. 1, pp. 597–625, 1994.

28. Yanakiev, D. and I. Kanellakopoulos, "Nonlinear Spacing Policies for Automated Heavy-Duty Vehicles", *IEEE Transactions on Vehicular Technology*, Vol. 47, No. 4, pp. 1365–1377, 1998.

29. Swaroop, D. and K. Rajagopal, "A Review of Constant Time Headway Policy for Automatic Vehicle Following", *IEEE Intelligent Transportation Systems*, Oakland, CA, USA, pp. 65–69, 2001.

30. Yanakiev, D. and I. Kanellakopoulos, "Variable Time Headway for String Stability of Automated Heavy-Duty Vehicles", *Proceedings of 34th IEEE Conference on Decision and Control*, New Orleans, LA, USA, pp. 4077–4081, 1995.

31. Broqua, F., "Cooperative Driving: Basic Concepts and a First Assessment of Intelligent Cruise Control Strategies", *DRIVE Conference*, Brussels, Belgium, pp. 908–929, 1991.

32. Stanger, T. and L. del Re, "A Model Predictive Cooperative Adaptive Cruise Control Approach", *American Control Conference*, Washington, DC, USA, pp. 1374–1379, 2013.

33. Besselink, B., V. Turri, S. H. van de Hoef, K.-Y. Liang, A. Alam, J. Mårtensson and K. H. Johansson, "Cyber–Physical Control of Road Freight Transport", *Proceedings of the IEEE*, Vol. 104, No. 5, pp. 1128–1141, 2016.

34. Ozkan, M. F. and Y. Ma, "Fuel-Economical Distributed Model Predictive Control for Heavy-Duty Truck Platoon", *IEEE International Intelligent Transportation Systems Conference (ITSC)*, Indianapolis, IN, USA, pp. 1919–1926, 2021.

35. Törnell, J., S. Sebben and D. Söderblom, "Influence of Inter-Vehicle Distance on the Aerodynamics of a Two-Truck Platoon", *International Journal of Automotive Technology*, Vol. 22, No. 3, pp. 747–760, 2021.

36. Hammache, M., M. Michaelian and F. Browand, "Aerodynamic Forces on Truck Models, Including Two Trucks in Tandem", *Proceedings of the SAE Technical Paper Series*, Detroit, MI, USA, pp. 50–67, 2002.

37. Eriksson, L., A. Larsson and A. Thomasson, "The AAC2016 Benchmark - Look-Ahead Control of Heavy Duty Trucks on Open Roads", *IFAC-PapersOnLine*, Vol. 49, No. 11, pp. 121–127, 2016.

38. Eriksson, L. and L. Nielsen, *Modeling and Control of Engines and Drivelines*, John Wiley & Sons, Chichester, 2014.

39. Kamal, M. A. S., M. Mukai, J. Murata and T. Kawabe, "Model Predictive Control of Vehicles on Urban Roads for Improved Fuel Economy", *IEEE Transactions on Control Systems Technology*, Vol. 21, No. 3, pp. 831–841, 2013.

40. Kamal, M. A. S., M. Mukai, J. Murata and T. Kawabe, "Ecological Vehicle Control on Roads With Up-Down Slopes", *IEEE Transactions on Intelligent Transportation*

Systems, Vol. 12, No. 3, pp. 783–794, 2011.

41. Borrelli, F., A. Bemporad and M. Morari, *Predictive Control for Linear and Hybrid Systems*, Cambridge University Press, Cambridge, 2017.

42. Ploeg, J., B. T. M. Scheepers, E. van Nunen, N. van de Wouw and H. Nijmeijer, "Design and Experimental Evaluation of Cooperative Adaptive Cruise Control", *14th International IEEE Conference on Intelligent Transportation Systems (ITSC)*, Washington, DC, USA, pp. 260–265, 2011.

43. Tapli, T. and M. Akar, "Cooperative Adaptive Cruise Control Algorithms for Vehicular Platoons Based on Distributed Model Predictive Control", *IEEE 16th International Workshop on Advanced Motion Control (AMC)*, Kristiansand, Norway, pp. 305–310, 2020.

44. Dunbar, W. B. and D. S. Caveney, "Distributed Receding Horizon Control of Vehicle Platoons: Stability and String Stability", *IEEE Transactions on Automatic Control*, Vol. 57, No. 3, pp. 620–633, 2012.

45. Kianfar, R., P. Falcone and J. Fredriksson, "A Control Matching Model Predictive Control Approach to String Stable Vehicle Platooning", *Control Engineering Practice*, Vol. 45, pp. 163–173, 2015.

46. Öncü, S., J. Ploeg, N. van de Wouw and H. Nijmeijer, "Cooperative Adaptive Cruise Control: Network-Aware Analysis of String Stability", *IEEE Transactions on Intelligent Transportation Systems*, Vol. 15, No. 4, pp. 1527–1537, 2014.

47. Huang, H., H. Guo, Q. Dai and H. Chen, "Nonlinear Moving Horizon Control for Following Vehicles in Truck Platooning", *Chinese Control And Decision Conference (CCDC)*, Shenyang, China, pp. 1732–1737, 2018.